Hochschule
Bonn-Rhein-Sieg
University of Applied Sciences

b-it Bonn-Aachen International Center for Information Technology

R&D Project

Semantic Mapping for Enhanced Localization in Indoor Environments

Allen Isaac Jose

Submitted to Hochschule Bonn-Rhein-Sieg,
Department of Computer Science
in partial fullfilment of the requirements for the degree
of Master of Science in Autonomous Systems

Supervised by

Prof. Dr.-Ing. Sebastian Houben
Deebul Nair, M.Sc.

September 2023

I, the undersigned below, declare that this work has not previously been submitted to this or any other university and that it is, unless otherwise stated, entirely my own work.

Date	Allen Isaac Jose

Abstract

Your abstract

Acknowledgements

Thanks to ....

Contents

1 Introduction **1**
- 1.1 Motivation . . . 1
  - 1.1.1 Topic of this RnD project . . . 1
  - 1.1.2 Relevance of the topic . . . 1
- 1.2 Challenges and Difficulties . . . 2
  - 1.2.1 Challenges . . . 2
  - 1.2.2 Difficulties . . . 2
- 1.3 Problem Statement . . . 2
  - 1.3.1 Aim of the Project . . . 2
  - 1.3.2 Research Question . . . 2

2 State of the Art **3**
- 2.1 2D SLAM . . . 3
  - 2.1.1 2D Mapping Methods . . . 3
  - 2.1.2 2D Localization Methods . . . 3
- 2.2 3D SLAM . . . 3
  - 2.2.1 3D Mapping Methods . . . 3
  - 2.2.2 3D Localization Methods . . . 4
- 2.3 Limitations of Previous Work . . . 4

3 Methodology **5**
- 3.1 Experimental Setup . . . 5
- 3.2 Evaluation metrics . . . 5

4 Comprehensive study of Selected algorithms **9**
- 4.1 QuadricSLAM . . . 9
  - 4.1.1 Summary . . . 9
  - 4.1.2 GTSAM . . . 17
  - 4.1.3 Code Explanation . . . 19
  - 4.1.4 Key insights . . . 24
- 4.2 OA-SLAM . . . 26
  - 4.2.1 Related works . . . 26
  - 4.2.2 Summary . . . 32
  - 4.2.3 Code Explanation . . . 33
  - 4.2.4 Key insights . . . 33
- 4.3 Comparative Evaluation of SLAM pipelines . . . 34

5 Evaluation and Results **37**
5.1 Experiment Description 37
5.2 Results 41

6 Conclusions **47**
6.1 Contributions 47
6.2 Lessons learned 47
6.3 Future work 47

Appendix A Design Details **49**

Appendix B Parameters **51**

References **53**

1

Introduction

- Brief description of SLAM in simple words.

1.1 Motivation

1.1.1 Topic of this RnD project

- What is the topic to be covered?
- Where can it be used?
- What do you hope to achieve with this study?

1.1.2 Relevance of the topic

- Why choose this topic?
- Contextual Background: Provide a brief overview of the broader context within which your research is situated
- How can it benefit? real-world applications?
- Impact of the topic
- Address existing gap
- Why your research is timely and relevant in the current context
- Supporting Previous Findings: If your research aligns with or supports previous studies, discuss how it reinforces the existing knowledge base and provides additional evidence.
- Emerging Trends: Explain how your research aligns with or responds to emerging trends or developments in the field.

- Interdisciplinary Connections: If your research bridges multiple disciplines, highlight the importance of cross-disciplinary collaboration and how it enriches the understanding of the research problem.(the connection between traditional multi-view geometry of computer vision and the deep learning domain)

1.2 Challenges and Difficulties

1.2.1 Challenges

- Existing problems. Acknowledge any challenges or limitations your research may face and how you plan to address them.
- What is required to solve the problem
- Data Availability and Collection: Discuss any potential challenges related to data availability, accessibility, or reliability. (dataset with GT object pose and GT trajectory information) (most papers deal only with qualitative comparisons than quantitative ones)

1.2.2 Difficulties

- Why is it difficult
- Potential obstacles
- occlusion of objects, dynamic objects, scale ambiguity in case of a monocular camera, data association problem, initialization problem.

1.3 Problem Statement

1.3.1 Aim of the Project

- What are we going to do in this project
- Methodological Approach: Briefly mention the methodology or approach you will use to achieve the objectives.
- If any Novelty and Innovation
- Generalizability of your findings.

1.3.2 Research Question

- What are we issues are being addressed in this paper
- Unanswered questions that your research aims to address
- Formulate the research questions or hypotheses that will guide your investigation.

2

State of the Art

2.1 2D SLAM

- Explain what all sensors are being considered - 2D LIDAR and camera in case of semantics onto 2D plane. odometry from wheel encoders.
- What is 2D SLAM and where is it used?

2.1.1 2D Mapping Methods

- Different types of maps being created - topological, metric(occupancy grid), semantic, hybrid
- Different mapping methods - hector slam, cartographer, GMapping, KARTO-SLAM, Fast-SLAM, 2d semantic mapping methods

2.1.2 2D Localization Methods

- Different localization methods - variants of Kalman filter, variants of particle filter
- Usage of 2d semantic maps for localization

2.2 3D SLAM

- Which all sensors - RGBD camera, 3D LIDAR, Stereo camera. Not focusing on 3D SLAM with only 3D LIDAR.
- What is 2D SLAM and where is it used?

2.2.1 3D Mapping Methods

- Different types of maps being created - dense(entire point cloud, or 3d octomap), semi-dense(orb keypoints, important features only), sparse(semantics of object enclosed in shapes like cuboid, ellipsoid)

- Different mapping methods - kimera, orbslam, RTAB, LSD-SLAM, Cubeslam, EAO slam, PlanarSLAM, KinectFusion, ElasticFusion, DTAM

2.2.2 3D Localization Methods

- Visual localization - as in cuboidal slam, rat-slam
- Keypoint based localization - as in orb slam

2.3 Limitations of Previous Work

- Why can't 2D SLAM be used in a dynamic environment?
- Problems with 2D localization.
- Size of the map to be stored.
- Time taken to create the map.
- Sensor inputs required for mapping.
- Time taken for localization.
- Online and offline map semantic processing.
- Computational power needed to process.
- Non-semantic maps cannot be used for semantic navigation. Cannot perform scene change detection.

3

Methodology

How you are planning to test/compare/evaluate your research. Criteria used.

3.1 Experimental Setup

- On YCBV test dataset available in BOP format.
- On the YCB dataset generated using blenderproc.
- On Kinova robotic arm for object pose detection.
  - How is data passed into the SLAM algorithm?
  - How is the output processed?
  - Metrics used for testing and comparison.
- Below mentioned are some of the publicly available dataset for the usecase.
  - TUM RGBD dataset [1] - ground truth odom, RGB image, depth image and accelerometer data are available. Can be used for trajectory error measurement.(here)
  - BOP dataset - ground truth camera pose, RGB image, depth image, ground truth object poses, object bounding boxes.(here)

3.2 Evaluation metrics

- Below mentioned are some of the evaluation metrics to test the **object pose errors**.
  - **Centroid error** - Measures the Euclidean distance between the actual object centroid and the estimated quadric centroid. For each object, this could be individually calculated to identify which has max and which has min deviation among all. Also, it can be calculated as the root mean square deviation of the estimated object centroid from the ground truth object centroid for all the objects. RMSE $E_{\text{cen}} = \frac{1}{n}\sum_{i=1}^{n}\sqrt{\left\|\mathbf{q}_j^{\text{t}} - \hat{\mathbf{q}}_j^{\text{t}}\right\|^2}$. The estimated centroid can be derived from the 3 elements of the last column of the dual quadric representation matrix of size 4x4. [2]

  - **Rotation error** - Measured as the angle between the rotation matrixes of ground truth and estimated object pose represented in unit quaternion format. This can be done by performing dot product operation on these quaternions and then converting it to angular format in radians.
  - **Volume error** - Measures the difference between the actual ground truth volume of the object and the estimated volume of the object by comparing the overlapping between them. To compute the actual volume of the object, we may need to use the available 3D cuboid representation of the ground truth objects. Then we need to perform Monte Carlo sampling to randomly sample points within the ground truth 3D cuboid and check how many of them lie within the estimated ellipsoid to get an idea of the overlapping percentage. Even though it may not give the exact quantity of the error, it can still represent the volume error which should be as low as possible.

- Below mentioned are some of the evaluation metrics to test the **camera pose or trajectory errors**.
  - **Trajectory deviation error** - Measures the 3D position error of the estimated trajectory and the actual trajectory. It can be calculated as root mean square deviation of the estimated pose from the ground truth pose. $\text{RMSEpos}_{\text{pos}} = \frac{1}{n}\sum_{i=1}^{n}\sqrt{\|\mathbf{x}_i^{x,y,z} - \hat{\mathbf{x}}_i^{x,y,z}\|^2}$. If the robot is moving in a plane, we can assume z=0 [2]. We can get the max and min deviation in the estimated trajectory from the ground truth trajectory along with the plot for deviation for each camera frame. Also, the root mean square deviation is computed.
  - **Rotation error** - Same metrics definition as that of rotation error in object pose error evaluation metric. We can plot the angular deviation plot for each camera frame. Average rotational error is computed.
  - **Trajectory similarity measurements** - Given a set of 3D points of the ground truth and the estimated trajectories, we can perform the similarity checking of those trajectories using Procrustes Analysis, Fréchet Distance, Chamfer Distance.

- Below mentioned are some of the evaluation metrics to test the **object initialization errors**.
  - **Uninitiated objects error** - This error is measured in terms of integer numbers which indicate how many objects in the environment were not mapped by the Quadric SLAM approach.
  - **Association error** - This error is also estimated in integers where it indicates the number of wrong associations of objects.
  - **Duplication error** - Measured in integers where it counts how many copies of the objects in the real world are duplicated in the created map.

- Trajectory error is mentioned as trajectory quality and Centroid & volume error are mentioned as landmark quality evaluation metrics in the main paper [2].

- Metrics such as centroid error, volume error, uninitiated objects error and orientation error as Match factor are mentioned in the master thesis by Kamil Kaminski [3].

- Below mentioned are some of the metrics to compare the **performance** of different object-oriented SLAMs.
  - **Size of stored map** - to compare how much space is needed to store the map containing the objects.
  - **Computational power needed** - This can be measured based on CPU, GPU, RAM usage system profile.
  - **Computation time** - How much time is required for a single step in the SLAM. That is, taking the image input and updating the internal parameters. Overall computation time and time taken for each functional block in the SLAM needs to be identified to check which operation consumes more time.

4

Comprehensive study of Selected algorithms

From the 3D semantic SLAM methods, we are selecting QuadricSLAM and OA-SLAM methods to look into the backend pipeline, understand the implementation details and identify the challenging sections within it. Also, the evaluation of such object-oriented SLAM methods are also performed.

4.1 QuadricSLAM

4.1.1 Summary

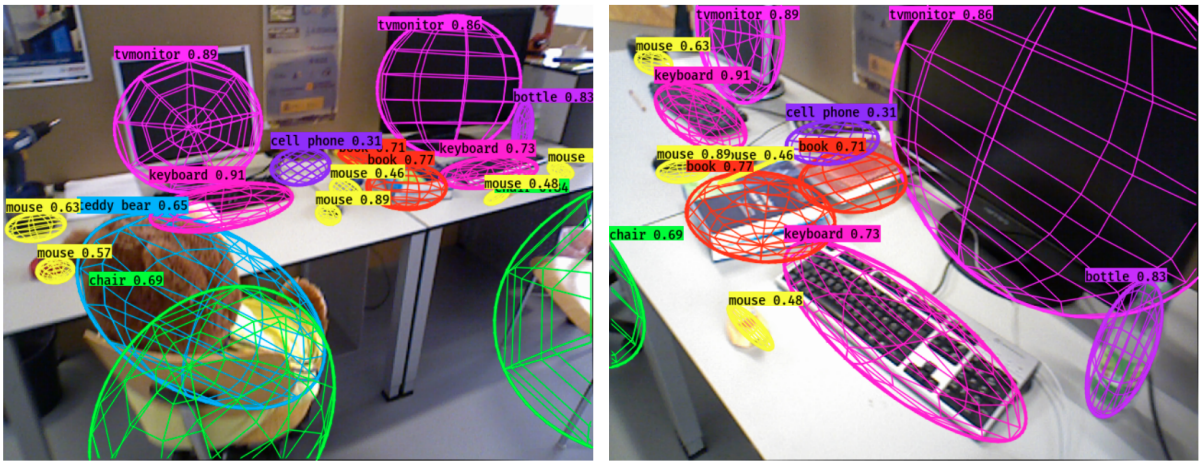

Figure 4.1: **QuadricSLAM**: Ellipsoids fitted on objects in image plane [4]

- The Quadric SLAM is a semantic SLAM approach where each object within the environment is represented using dual quadrics whose parameters are estimated and optimised using multi-view geometry.
- The optimisation is based on the 2D bounding box generated for each object observed at different view points. This object detection method also helps to add semantic label to each object.

- SLAM involves performing mapping and robot pose estimation in a combined fashion. Here the robot camera poses and the quadric parameters are estimated using underlying factor graph based back-end. The odometry errors in the factor graph could be reduced through the loop closure which is aided by re-observing the quadric representation of the object at different view points. Thus both the odometry and the observation are aiding to minimize the errors of each other.

- In the initial paper released by the authors [2], a monocular perspective camera was used to input RGB images to the front-end of the framework without any depth information.

- The quadric used in this application is ellipsoid because its a closed surface. It can capture the position(3 parameters), radius or size(3 parameters) and orientation(3 parameters) of the object in the 3D world. This kind of representation can help to reduce the memory required to store the dense 3D representation of the surface of the object and at the same time serves all the basic purposes like object pose estimation, localization, semantic navigation and planning tasks.

- The following section explains about the mathematics behind dual quadric representation. The section is a summarized version of the content in section 3 of the Quadric SLAM paper [2].

- For each view of an object, a 2D bounding box is generated with 4 corners x_1, x_2, x_3 and x_4. Each one can be represented using a 3D homogeneous vector.

- Further, the 4 edges of the bounding box l_1, l_2, l_3 and l_4 can be represented as a cross product of these corner points. $l_1 = x_1 X x_2, l_2 = x_2 X x_3, l_3 = x_3 X x_4$ and $l_4 = x_4 X x_1$.

- The lines drawn from the camera center to each of the four corner points can back-project the four edge lines into four 3D planes. The equation of the 3D plane can be written as $\pi_i = P^T l_i$ where i is the index of the 2D edge for which the 3D plane is generated. P is the camera projection matrix, P = K[R t] where K is the intrinsic parameter matrix of size 3x3 and R and t are the extrinsic parameter matrix of the camera of size 3x4. Therefore P is a matrix of size 3x4 and the resultant 3D plane π_i is a 4D homogeneous vector.

- Thus a single view can create a constrained 3D space enveloped by four 3D planes. Since we don't have an enclosed 3D region from a single view, we may need multiple views to further constrain the object's shape and orientation.

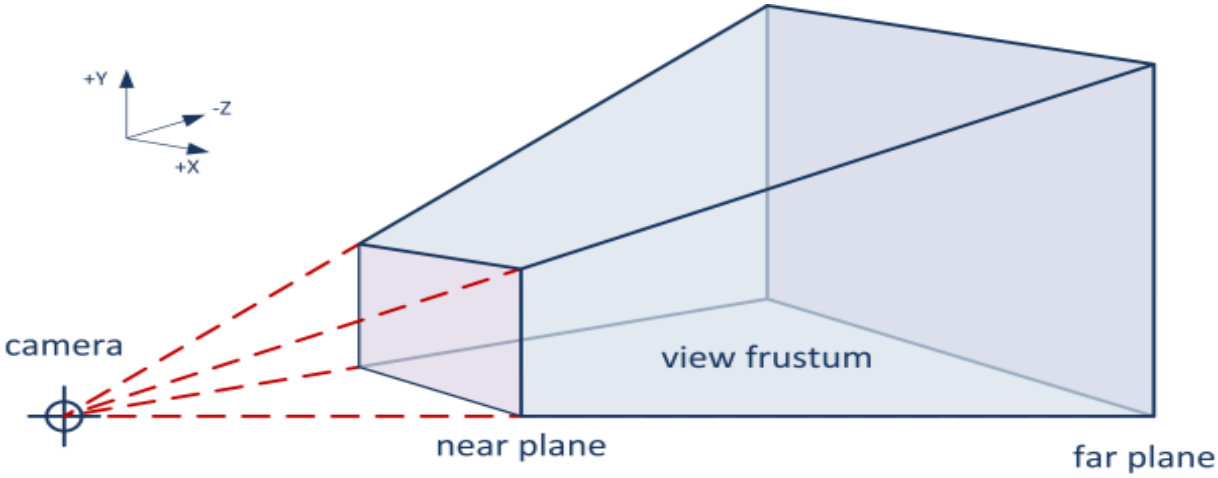

Figure 4.2: Back projection of 2D bounding box [ref]

- In the above figure 4.2, we can see the bounding box which is represented as the near plane which is back-projected to infinity. The view frustum area is the most probable area where the object can be located. To form a closed region from these 3D view frustums, we need at least 3 views which can be seen in the figure 4.3 below.

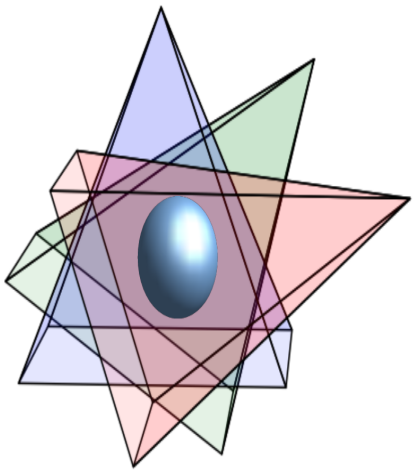

Figure 4.3: Closed region by 3 view frustums

- The next important concept is what and how to represent a quadric. A quadric Q is a 3D surface that is characterized by a set of points x on the surface that satisfies the equation $x^T Q x = 0$. Q is a 4x4 symmetric matrix.
- The same equation can be rewritten in terms of tangential planes that passes through each of these points that can create an closing envelope around the surface. $\pi^T Q^* \pi = 0$. Q^* is called as dual

quadrics or dual representation of the quadric which is calculated by $Q^* = Q^{-1}$ if Q has an inverse or $Q^* = adjoint(Q)$.

- Since Q^* is a symmetric 4x4 matrix, there are 10 unique elements. Three for centroid, three for size or radius, three for orientation and one for scaling factor which is usually kept constant as -1. So only need to optimize for 9 parameters. Q^* can be represented as $Q^* = TQ_0^*T^T$ where Q_0^* is the representation of an ellipsoid centered at origin and T is the homogeneous transformation matrix of size 4x4 involving a rotation and translation parameter [R t] to transform the ellipsoid from origin.

$$Q_0^* = \begin{bmatrix} r_1^2 & 0 & 0 & 0 \\ 0 & r_2^2 & 0 & 0 \\ 0 & 0 & r_3^2 & 0 \\ 0 & 0 & 0 & -1 \end{bmatrix}$$

- The parameters r_1, r_2 and r_3 governs the size or radius of the ellipsoid. The orientation and centroid parameters are incorporated as rotation and translation parameters in the homogeneous transformation matrix T. After matrix multiplication, the matrix Q^* turns into a transformation matrix where the centroid is the last column of Q^* as a homogeneous 4x1 vector. The orientation parameters pitch, yaw, roll has to be extracted from the first 3x3 dimension of the dual quadric matrix.

- The above concept of $\pi_i^T Q^* \pi_i = 0$ represents an 3D equation. However the bounding box observations we obtained from the detectors are in 2D. We have to convert from quadrics to conics which is ellipsoids to ellipses in this case. The dual conics C^* can be written as $C^* = PQ^*P^T$ where the 3D ellipsoid Q^* is projected onto the 2D image plane using the camera projection matrix P mentioned before.

- The definition of quadrics also remains same for conics $x^T Cx = 0$ where x is now replaced with 2D points. And as tangential planes exists for points in 3D, tangential lines exists for points in 2D. Hence $\pi^T Q^* \pi = 0$ for quadrics could be replaced by $l^T C^* l = 0$ for conics where C^* is the dual conic representation and l is the set of tangential lines.

- Substituting the expression for dual conics in the above equation yields, $l^T PQ^* P^T l = 0$.

- Per detection of an object from a view point, the bounding box generates 4 lines which can act as 4 constraints on the dual quadrics. For dual quadrics Q^*, there are 9 unknown parameters and atleast 3 observations from different view points are needed to generate a solution for the same.

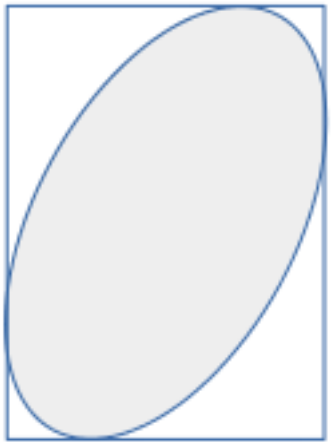

Figure 4.4: Four tangential lines to the object conic ellipse

- Internally, the quadricSLAM has the virtual representation of the 3D environment and when the camera pose comes back to already mapped object, the 2d view of the 3D object is projected onto the image plane as in figure 4.1. The concept is similar to the image 4.5 below except that in our case, the 3D object is ellipsoid and the 2D projection is ellipse.

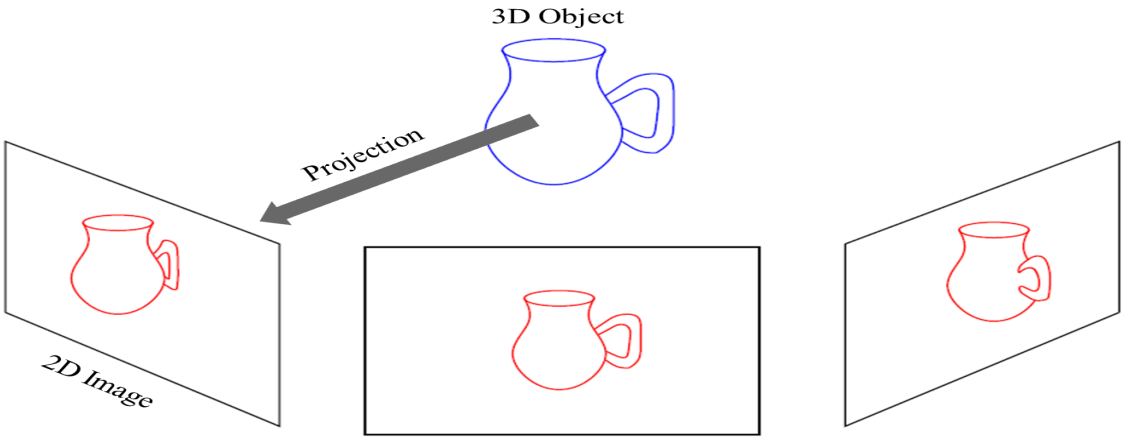

Figure 4.5: 3D virtual scene to 2D image plane projection [ref]

- The following section explains about the mathematics behind using the dual quadric representation in SLAM backend for optimization and corrections. The section is a summarized version of the content in section 4 of the Quadric SLAM paper [2].

- To define the factor graph, we define certain parameters for the odometry and observations:

  - A set of robot camera poses X = $\{x_i\}$ where i is the index of the pose at which a particular observation is made.
  - A set of landmarks Q = $\{q_j\}$ where q_j indicates the dual quadric representation for the object j.
  - A set of observations U = $\{u_i\}$ where u_i is the odometry data available via wheel odometry or visual odometry.
  - A set of lines L = $\{l_ijk\}$ where k ranges from 0 to 4. l_ijk denotes the line k of the bounding box for object j being viewed at pose i.

- The conditional probability distribution could be written as:

$$P(X, Q \mid U, L) \propto \underbrace{\prod_i P\left(\mathbf{x}_{i+1} \mid \mathbf{x}_i, \mathbf{u}_i\right)}_{\text{Odometry Factors}} \cdot \underbrace{\prod_{ijk} P\left(\mathbf{q}_j \mid \mathbf{x}_i, \mathbf{l}_{ijk}\right)}_{\text{Landmark Factors}} \tag{4.1}$$

- This modelled representation of factor graph tries to find the optimal solution for poses X^* and landmarks Q^* for a given set of odometry observations U and detected bounding box lines L. In other words, we are trying to find maximum a posteriori values for X and Q through non-linear optimization strategies.

- The equation involving dual quadric parameter($l^T P Q^* P^T l = 0$) can be optimized through least squares method. $\mathbf{q}_j^* = \text{argmin}_{\mathbf{q}_j} \sum_{ik} \left\| \mathbf{l}_{ijk}^\top \mathbf{P}_i \mathbf{Q}_{(\mathbf{q}_j)}^* \mathbf{P}_i^\top \mathbf{l}_{ijk} \right\|^2$. This maximizes the probability distribution for landmark factors in the above equation (1).

- Further, maximizing the conditional probability distribution (1) could be simplified by minimizing the negative log of the probability. Thereby, the multiplication terms turns to addition and turning the entire SLAM problem into a least squares problem.

- The factor graph is solved using Levenberg-Marquardt optimization strategy for non-least squares problem in this case and GTSAM [5] is the library being used in the backend for efficient computations by taking advantage of sparse nature of the jacobian matrixes.

- If depth information is available, it could also be added to the least squares problem as an extra error term that can represent additional knowledge of the problem which can be added as a factor in the factor graph.

$$X^*, Q^* = \underset{X,Q}{\text{argmin}} \underbrace{\sum_i \left\| \mathbf{e}_i^{\text{odo}} \right\|_{\Sigma_i}^2}_{\text{Odometry Factors}} + \underbrace{\sum_{ijk} \left\| \mathbf{e}_{ijk}^{\text{quadric}} \right\|_{\Lambda_{ijk}}^2}_{\text{Quadric Landmark Factors}} + \underbrace{\sum_{ij} \left\| \mathbf{z}_{ij} - \mathbf{T}_i \left(\mathbf{q}_j^{\text{t}} \right) \right\|_{\Omega_{ij}}^2}_{\text{Relative Position Factors}} \tag{4.2}$$

- Each of the three factors are trying to minimize the odometry error, dual quadric parameters error and centroid of the quadric (last column of dual quadric) error respectively. In the third term, z_{ij} is

the observed depth of the object j at pose i and $T_i(q_j^t)$ is transforming the centroid from last column of dual quadric representation from world coordinate to the robot coordinate at pose i. So the last term is for centroid correction.

- Another task is the variable initialization for robot poses x_i and dual quadrics q_i. x_i is initialized with the help of odometry data available from wheel odometry or visual odometry and q_i is initialized as a identity matrix of size 4x4.

Orientation Factor

- The same authors later came up with a continuation of this work to incorporate prior knowledge of the world to better orient the quadrics within the environment using orientation constraints [6]. The prior knowledge is that we need to assign each object class to one of the category such as Horizontal, Vertical or Unassigned. This corresponds to what is the normal pose of the object in relation with gravity. For example, a chair can be Vertical and a laptop can be Horizontal.

- Further, the major axis of the quadric is aligned close to z-axis(vertical line) or close to perpendicular to z-axis(horizontal line) based on the prior knowledge of the normal poses of the objects.

- To find the major axis, eigen values are calculated from the dual quadric representation involving only the rotation components and eigen vector corresponding to the largest eigen value is identified. Further, a cosine similarity between this vector and the z-axis is calculated.

- This value should be optimized towards 1(cosine similarity of 1) if the prior knowledge of the object pose is Vertical(gravity, major axis and z-axis in same direction). And the value should be optimized towards 0(cosine similarity of 0) if the prior knowledge of the object pose is Horizontal(major axis is perpendicular to gravity and z-axis).

- To implement this in factor graph, the problem is made into a least squares problem and added as a factor to the factor graph. To the equation (2), a fourth factor is added as orientation factor.

$$\underbrace{\sum_{j} \|g\left(l_j\right) - c_j\|^2_{\sigma_j}}_{\text{Orientation Factors}} \tag{4.3}$$

- c_j is the cosine similarity value being calculated and $g(l_j)$ is the actual expected cosine similarity for the particular label l of the object j which can be 0 for Horizontal and 1 for Vertical.

- One of the problem of this approach is that, we need to assign each known class to one of the category such as Horizontal, Vertical or Unassigned. And, in the example which they have shown, they assigned book to be horizontal which can be a wrong assumption as books kept in shelf are in vertical orientation.

- This approach of adding the fourth orientation factor is not implemented in the available code of Quadric SLAM.

Sensor Model

- In the final paper released by the same authors in 2019 [4], they have added a sensor model to correct the errors in the predicted 2D bounding box of partially observable objects. We need to only consider the conic/ellipse part of the object within the image plane.

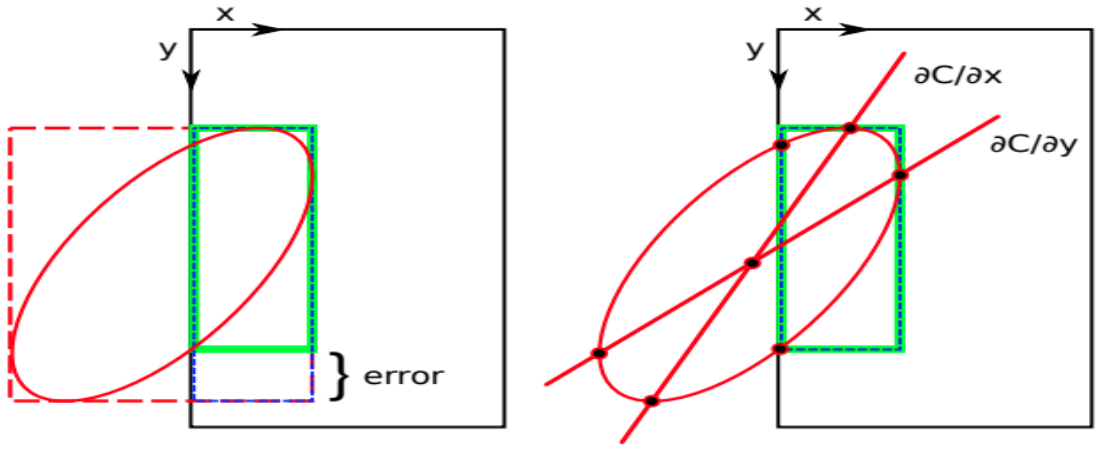

Figure 4.6: **Left**: The dotted red square is the predicted bounding box by the detector. Green square is the required bounding box. Violet is the error. **Right**: Error is removed through conic extreme x, y parameters [4]

- In the above figure, the black box is the image viewed by the robot and only a part of the conic of the object is visible within the image plane. Normally, the edges of the bounding box is truncated based on the edges of the image plane. And this resulted in the error component depicted by violet color where the object conic is absent.

- To reduce this geometric error, the bounding box within image plane is cropped using the conic extreme x and y parameters. For this, 4 points representing extreme points of the conic are selected along with the points that are intersecting between the conic and the 2D bounding box. All the points that lie outside the image plane are removed and from the remaining points within the image plane, the max and min values of x and y are determined which are used to create the accurate green 2D bounding box.

- The results of the experiments showed that this feature significantly improved the estimated trajectory and the quadric mapping in terms of reduced trajectory and landmark quality errors.

- The previously used error term in Quadric Landmark Factor was an algebraic one. That is, minimizing $\mathbf{q}_j^* = \text{argmin}_{\mathbf{q}_j} \sum_{ik} \left\| \mathbf{l}_{ijk}^\top \mathbf{P}_i \mathbf{Q}_{(\mathbf{q}_j)}^* \mathbf{P}_i^\top \mathbf{l}_{ijk} \right\|^2$. This is replaced by the geometric error proposed by the new sensor model, $\left\| \mathbf{b}_{ij} - \boldsymbol{\beta}_{(x_i,q_j)} \right\|^2_{\Lambda_{ijk}}$. Here, b_{ij} is the bounding box observed for object j at robot pose i. And $\boldsymbol{\beta}_{(x_i,q_j)} = BBOX(C_{ij})$ is the expected geometrically corrected bounding box for the conic C of the object j observed at pose i. $C = adjoint(C^*) = adjoint(P_i Q_j^* P_i^T)$ where P_i is the camera projection matrix at pose i and Q_j^* is the dual quadric representation of the object j.
- The 2D object detector used in the experiments is YOLOv3.

Variable Initialization

- In the final paper of Quadric SLAM [4], another initialization method for quadrics are proposed. Using the dual quadric representation of quadric $\pi^T Q^* \pi = 0$, we can create a linear set of equation which can be solved using SVD if atleast 3 views for the same object quadric is observed. The last column of decomposed matrix V gives the solution for the equation. The translation parameters can be obtained from the last column and the orientation parameters can be obtained from the first three columns of the solved Q^* matrix. The size is extracted from the eigen values. [4]

4.1.2 GTSAM

- GTSAM [5] library is used to build the factor graph backend for QuadricSLAM and performs as incremental solvers. The robot pose and the dual quadric matrix are represented as nodes which are the latent variables that needs to be estimated. The pose nodes are constrained by the odometry factors and the pose-quadric nodes are constrained by the bounding box factors.

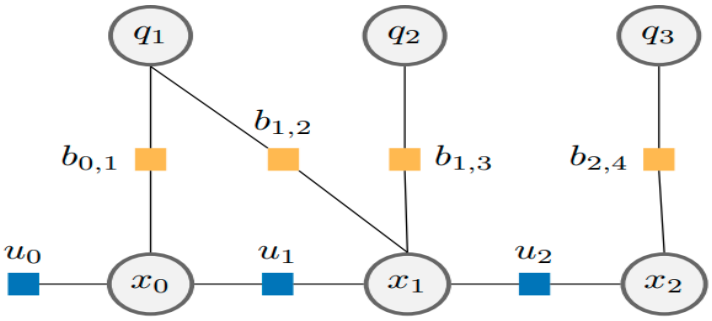

Figure 4.7: **Factor Graph of QuadricSLAM**: odometry factors in blue, quadrics bbox factors in yellow [6]

- In the above figure, it can be seen that the quadric q_1 is observed from two robot poses x_0 and x_1. As the same object is observed from different poses, it adds better constraint to optimize the quadric parameters. Actions(in this case robot motion) introduces uncertainty whereas the observations (in this case the bounding boxes of detection) helps to reduce the uncertainty in the pose graph.

- Another important constraint in factor graph is loop closure constraint. Using the image or quadric features, when the robot detects that its in a pose which was visited at a previous point in time, it can create a loop closure constraint which can help to reduce the overall error in the factor graph. This is also a field of challenge where we need to verify or make sure that the features are qualified enough for a loop closure to avoid false positive loop closure detection which can have a bigger negative effect on the factor graph.
- The author's of QuadricSLAM, extended the GTSAM functionalities by creating another library called gtsam_quadrics which handles quadrics related functions.
- Some of the important functions used in QuadricSLAM are:
  - gtsam.symbol - used to symbolically represent the robot pose and quadric variables as nodes within the factor graph.
  - gtsam.noiseModel.Diagonal.Sigmas - can be used to define a noise model which is added into the factor graph when an odometry measurement or observation is used to add a constraint between 2 variables or nodes. It indicates with how much uncertainty, we are adding the measurement to the factor graph.
  - gtsam_quadrics.ConstrainedDualQuadric - used to represent the quadric based on the given the input parameters like rotation, translation, radii matrixes as it has different constructors.
  - gtsam.NonlinearFactorGraph - Used to initialize a factor graph onto which the robot pose and quadrics are added as latent variables along with the odometry and bounding box measurements as factors with an assosciated noise model.
  - gtsam.Cal3_S2 - to generate calibration matrix
  - gtsam.Pose3 - create a 3D pose of rotation and translation matrix based on the input provided.
  - gtsam.Rot3 - create a 3D rotational matrix.
  - gtsam.PriorFactorPose3 - to generate the initial robot pose with a prior noise model which is added to the factor graph.
  - gtsam.BetweenFactorPose3 - to add the odometry measurement factor between two robot poses with a odometry noise model which is added to the factor graph.
  - gtsam_quadrics.BoundingBoxFactor - to add the bounding box observation as a factor between a robot pose and a quadric which is added to the factor graph. Bounding box noise is also assosciated with the function.
  - gtsam_quadrics.QuadricCamera.project - given a dual quadric matrix and robot pose, it will generate the 2D view(conic) of the quadric in the image plane from which using the function bounds(), we can obtain the 2D bounding box virtually.
  - gtsam.LevenbergMarquardtOptimizer - Given the factor graph and a initial estimate for the robot poses and quadric latent variables, a non-linear optimization is applied on the graph to get the results.

- It can be seen that there is a noise model attached to every odometry, observation and prior measurement factor. This creates the uncertainty region for adjusting the edges between the nodes during bundle adjustment. If the noise model is set to 0, it means the measurement is taken with 100% accuracy and then the node(in this case, the camera pose or the object pose) will be fixed or immovable.

4.1.3 Code Explanation

Overall Framework

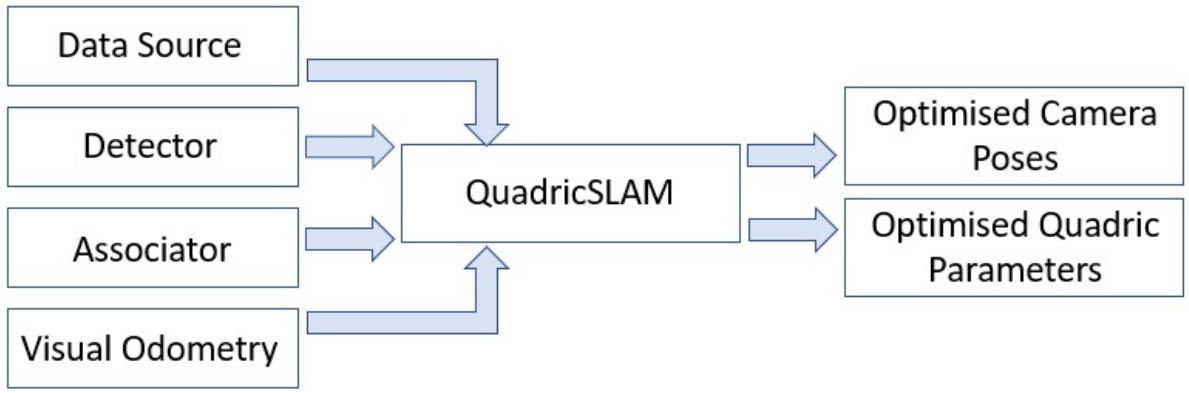

Figure 4.8: QuadricSLAM framework

- The above figure depicts the general functional framework of QuadricSLAM. QuadricSLAM is implemented as a class which takes in the class objects of data source, detector, associator and visual odometry. And what we get out of QuadricSLAM is the optimised camera poses and quadric parameters which can be used to create the map. Each component is explained below.

Data source

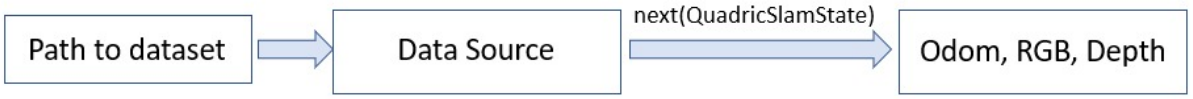

Figure 4.9: Data source

- Used to either access an available dataset(acts as a dataloader) or provide the live data to the QuadricSLAM algorithm. The data include odometry, RGB image and depth image. These data is retrieved by QuadricSLAM by calling the next() function of data source.

- The odometry should be converted from quaternion or transformation matrix format to SE3() pose representation in spatial math.
- Datasource also maintains an internal counter to step through each data in time and also checks for data read completely or not.
- Depthscaling factor and RGB calibration parameters are also stored here. Images are calibrated before passing into the QuadricSLAM.
- If using a live data, then the configuration of the data source can be defined in the init() function. If using an available dataset, then the path to the dataset is to be passed into here.

Detector

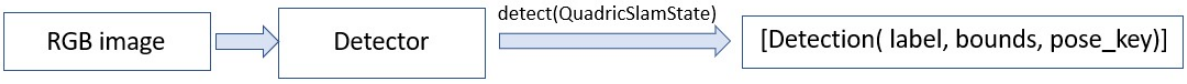

Figure 4.10: Detector

- Used for detecting objects in each RGB image frame. The detect() function outputs the list with elements of object type Detection which contains label of the object, list of 4 values of the bounding box(x,y of top-left and bottom-right corners) and the pose_key which indicates at which pose number the current detection is made.
- The default detector used here is the detectron2 Faster-RCNN. A pretrained model on certain labels is used here. Only those objects are detected.
- In the experiments which we are going to perform on BOP dataset, we are going to avoid the usage of a detector and instead provide the bounding box directly available from the dataset. This will help us to evaluate the performance of QuadricSLAM given the noise from the bounding box is kept minimum.

Associator

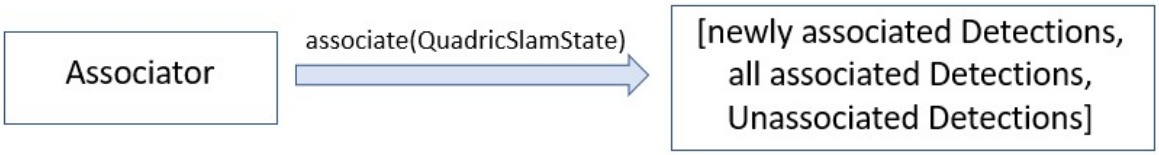

Figure 4.11: Associator

- Data Associator takes the detections made in the current state and all previously unassosciated detections and used it to compare with previously assosciated detections to decide whether to match the unassosciated detection with a previously assosciated detection(same quadric key to both detection) or to treat the detection as a new object(new quadric key to the detection).
- Basically, it decides whether a detection should be given an existing quadric key or create a new quadric key for it.
- The decision is based on the Intersection Over Union(IOU) value between the detection and an existing quadric. With respect to the current robot pose, all the existing quadrics within the factor graph is projected in 2D plane as a enclosing bounding box. For each current detection bounding box, we are comparing its overlap with each bounding box generated within the map of QuadricSLAM. If the overlap is below a certain threshold, then treated as a new object with a new quadric key. Otherwise, assosciated to an existing object with the quadric key of the overlapping quadric.
- In the init() function, we can specify threshold above which an assosciation should be made.
- The associate() function outputs the list of the newly associated detections(objects for which a new quadric has been created in the current step), updated list of associated detections(all objects that has been assosciated with a quadric key), updated list of unassociated detections(objects that doesn't have a quadric key - usually passed as an empty list).

Visual Odometry

Figure 4.12: Visual Odometry

- Could be used to generate the odometry from current and previous RGBD image. Usefull when no odometry information is available.
- Here, RgbdOdometry from CV2 library is being used. The current and previous RGB images are converted intro gray scale and provided as input along with their depth images to compute the odometry.
- odom() function returns the odometry value.
- Other visual odometry approaches suggested by the authors are ORB-SLAM2 with loop closure disabled or Kimera VIO(Visual Inertial Odometry) to get a less noisy odometry value.

Main code

- There are two ways to initialize a quadric. initialise_quadric_ray_intersection() and initialise_quadric_from_depth().

- In initialise_quadric_ray_intersection(), the translation and rotation of the poses at which a particular object is seen is used to project rays into 3D space and using least squares method to find the closet converging point which is a good approximation of the quadric centroid. The initial orientation and size of the quadric is random. In the code, the size is set to (1, 1, 0.1).

- In initialise_quadric_from_depth(), the quadric can be initialized from a single view or image. To estimate centroid, the z coordinate is calculated as the mean of the depth of points within the bounding box of detection. x and y coordinate are calculated as a calibrated value representing the centre point of the bounding box. The x,y radii of the quadric is calculated as a calibrated value of the height and width of the bounding box. The z radii is assumed to be a predefined object depth of 0.1. The orientation of the quadric can be estimated using the rotation, translation of the camera pose and the quadric centroid through gtsam.PinholeCameraCal3_S2.Lookat() function.

- There are two modes of optimization. Optimization in a batch or in an incremental way. If its set to true, then the optimization of the unknown variables occur only at the end of processing all the images. If false, then the optimization runs along with each detection step.

- There are 3 noise models used in this application. One for the prior noise which is added along with the initial pose of the robot. Another one for odometry measurement noise which is added to the constraint between two robot pose variables. Third one for bounding box noise which is added for the constraint between a robot pose and the observation measurement which is a bounding box. This noise is due to the instability of bounding box being generated for an object which is evident for small objects.

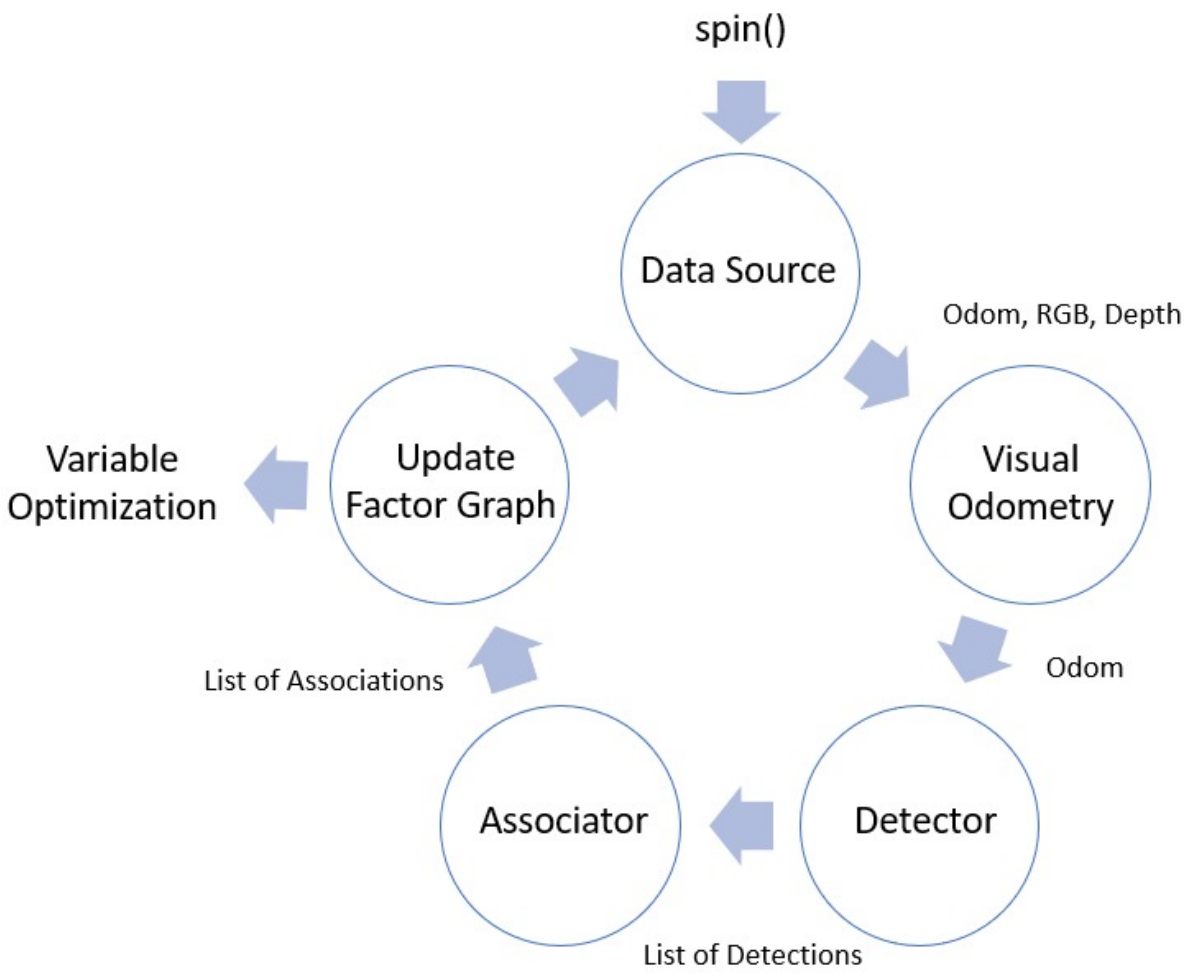

Figure 4.13: spin() function of QuadricSLAM

- The above figure 6 depicts the main operation of the QuadricSLAM which is the spin() function.
- The next() function of the datasource returns the current odom, RGB and depth.
- If there is no odom data, a visual odometry method could be used to generate the odom data.
- The detector takes in current RGB image and outputs a list of detections with information about the label, bounds and pose_key for each detected object. detect() function is used.
- The associator takes these detections and use IOU method to identify whether its an new object or an existing object in the graph. All the associations and unassociations are outputed by the associate() function.
- Based on the new pose and quadric information, the non linear graph is updated.

- This cycle of process continues until the dataset is completely processed.
- Based on the optimization batch setting that have been set, the unknown variables are either optimized at the end of processing all the dataset or done in an incremental fashion during each cycle.
- The values to be recorded after running the algorithm are state.estimates - which has the initial guess of the quadrics and the poses onto which the non-linear graph perform optimisation and state.labels - which has the actual label for the quadric key which we can use for evaluation purposes. Since, objects of same class appears multiple times within the graph, we cannot just use the actual label within the graph. So they are represented by a random number and this is stored in the state.labels.

4.1.4 Key insights

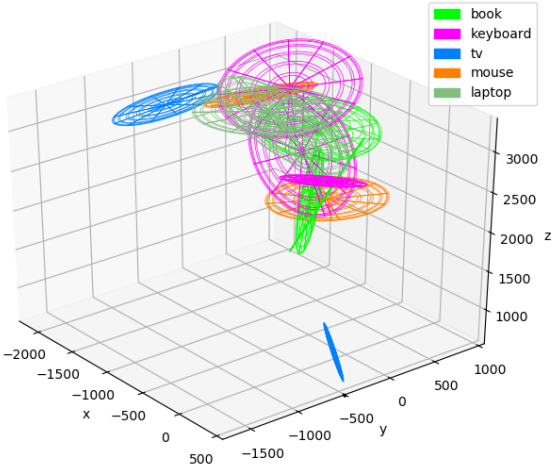

Figure 4.14: Batch optimization

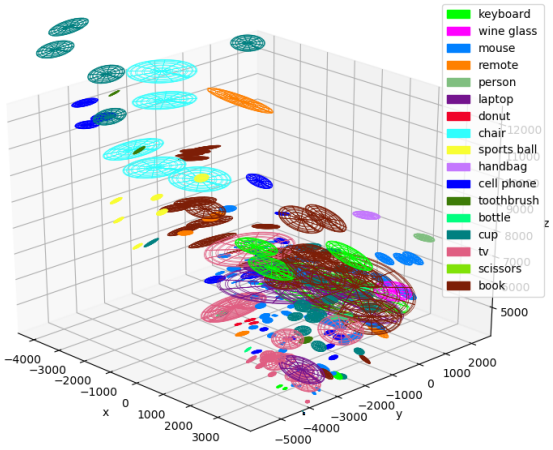

Figure 4.15: Incremental optimization

- The above plots represent the quadric representation of the freiburg1_desk scene of TUM RGBD dataset. In figure 4.14, the optimization of the factor graph is performed only at the end of reading the entire dataset(batch optimization). And the initial guess of the odometry value is the same as that of the provided ground truth odometry as we didn't used any explicit odometry estimation algorithm here. Because of that, the data association in each step of the data performed well in associating quadrics that belong together and thus generating 14 detected objects or quadrics in the end. Whereas in incremental optimization approach (figure 4.15), at each step, based on the initialized quadric from a single detection and the ground truth odometry, the factor graph is optimized. Thus the actual ground truth odometry is pulled to a wrong position to compensate for the noisy quadric detected. And this error accumulates over each time step and each detections of the same object in each data step appears at different locations in environment. This is the data

assosciation problem in QuadricSLAM that leads to duplication. Thus 236 quadrics are generated in the end as most of the detections of the same object couldn't be assosciated together.

- Another observation is that, since a single detection is used to generate a quadric, the uncertain predictions of the detector will generate some non existing objects due to the wrong label prediction. In the figure 4.15, objects like person, sports ball were not present in the environment. There should have been a counter to detect the number of times a particular label appears for a quadric and the final label should the most occurring one. This is possible only if the data assosciation problem is solved.

Benefits

- Geometric SLAM approaches utilised features like ORB [7], lines [8], planes [9] to represent the environment. But they lacked the semantic information for these geometrical features. And these features were used only to estimate the robot pose and create a dense point cloud of the environment. Whereas in Quadric SLAM, the knowledge of semantic label of the geometric represented as a quadric can help in loop closure and creation of a semantically enriched object-oriented map.

- As compared to SLAM++ [10] approach where prior knowledge of CAD models are used to represent the objects when they are detected, the Quadric SLAM doesn't require priors. For example, there can be different variations of chair and in SLAM++, it would be represented using the same CAD model of chair which can affect the mapping accuracy. In Quadric SLAM, the position, size and orientation could be accurately estimated from multiple views of the chairs thereby producing quadrics of different parameters for each type of chair.

- In SemanticFusion [11], each point in the point cloud is having a label and the 3d object reconstruction from the dense point cloud is performed as a post-processing step. In the proposed Quadric SLAM approach, the object representation as quadrics(mapping) is performed in an online fashion. Also, the sparse representations can help in easier storage of the map. For example, the 9 parameters of the dual quadric could be saved as a XML file.

Challenges

4.2 OA-SLAM

4.2.1 Related works

4.2.1.1 ORB-SLAM2

4.2.1.2 Structure Aware SLAM using Quadrics and Planes [12]

- As a continuation of quadricSLAM, Sünderhauf et. al. also looked into extracting planes from the environment which can act as an extra constraint combined with the feature points within the factor graph [12].
- This concept of infinite planes was first introduced into factor graphs as a least-squares optimization problem in the paper by Kaess [9]. And later, Taguchi et. al. presented a SLAM method where a combination of planes and points can be used to register 3D data, since a single plane can be used to replace a lot of inlier 3D points which can help in faster computations and compact representations. [13]
- In this work, planes are also considered as an important feature which is the most common feature occurring in indoor environments. A plane can represent a big region of the environment, especially in cases where there are very few objects within the environment to be mapped and used as anchors.
- These planes can be used to create three additional constraints. Constrain between the points lying on the plane and the plane parameters. Constrain between the object and the supporting plane parameters. Constrain between two planes.
- The following section explains about the mathematics behind quadric and plane representations along with how the constraints can be added to the factor graph as a non-linear least squares problem. The section is a summarized version of the content in section 3 of the "Structure Aware SLAM using Quadrics and Planes" paper [12].
- From the previous section on QuadricSLAM, we have seen that the closed-form equation of quadric with tangential planes is given by $\pi^T Q^* \pi = 0$ where Q^* is called as dual quadric representation. There are 9 unique elements within this symmetric matrix that needs to be estimated through error minimization. So the error vector generated is 9 dimensions.

$$\mathbf{Q}^* = \mathbf{T}_Q \mathbf{Q}_c^* \mathbf{T}_Q^T = \begin{bmatrix} \mathbf{R} & \mathbf{t} \\ \mathbf{0}^T & 1 \end{bmatrix} \begin{bmatrix} a^2 & 0 & 0 & 0 \\ 0 & b^2 & 0 & 0 \\ 0 & 0 & c^2 & 0 \\ 0 & 0 & 0 & -1 \end{bmatrix} \begin{bmatrix} \mathbf{R}^T & \mathbf{0} \\ \mathbf{t}^T & 1 \end{bmatrix} \tag{4.4}$$

- Since we are fixing the quadric to be ellipsoid in this application, the dual quadric representation Q^* could be written as 4.4. T_Q is the transformation matrix that transforms the ellipsoid from its origin by rotating and translating it. Q_c^* is the ellipsoid located at the origin with radius a,b and c. The last element of Q_c^* is made -1 to represent the dual quadric matrix as an ellipsoidal equation.

$$\mathbf{Q}^* = \mathbf{T}_Q \mathbf{Q}_c^* \mathbf{T}_Q^T = \begin{bmatrix} \mathbf{R} & \mathbf{t} \\ \mathbf{0}^T & 1 \end{bmatrix} \begin{bmatrix} \mathbf{L}\mathbf{L}^T & \mathbf{0} \\ \mathbf{0} & -1 \end{bmatrix} \begin{bmatrix} \mathbf{R}^T & \mathbf{0} \\ \mathbf{t}^T & 1 \end{bmatrix} \quad \text{where} \quad \mathbf{L} = \begin{bmatrix} a & 0 & 0 \\ 0 & b & 0 \\ 0 & 0 & c \end{bmatrix} \tag{4.5}$$

- Further, to make sure that the first 3 diagonal elements of the Q_c^* matrix are positive eigen values during optimization process in factor graphs, the equation 4.4 is updated to 4.5 so that it guarantees positive values.

- Now updation of Q^* means updating T and L where T is the transformation matrix of 6 parameters(3 rotation and 3 translation) and L is a diagonal matrix with 3 parameters(a, b, c scale parameters). Thus the 9 dimension error can be split into 6-dim and 3-dim errors for efficient computation.

$$\mathbf{Q}^* \oplus \Delta\mathbf{Q}^* = (\mathbf{T}, \mathbf{L}) \oplus (\Delta\mathbf{T}, \Delta\mathbf{L}) = (\mathbf{T} \cdot \Delta\mathbf{T}, \mathbf{L} + \Delta\mathbf{L}) \tag{4.6}$$

- The updation of quadric parameters in Q^* can be simplified as in equation 4.6. The Δ values indicate the update value. In the case of L, the updation operation is addition based on the first 3 values of the 9 dim error vector and in case of T, it needs to perform the transformation operation for the updation based on the last 6 values of the 9 dim error vector.

- This representation of Q^* in terms of T and L also helps to add initial prior information about the properties of the object into the factor graph. The size info can be initialized in L matrix and the rotation and translation info can be initialized in T matrix.

- Next, we have to represent the planes in mathematical form. Inspired by the work on infinite planes by Kaees [9], an infinite plane is represented by normalised homogeneous coordinates $\pi = \begin{bmatrix} a & b & c & d \end{bmatrix}^T$ to have a compact representation. n is the normal vector $\mathbf{n} = \begin{bmatrix} a & b & c \end{bmatrix}^T$ and d is the distance to the origin. This normal vector can be optimised using the rotation matrix algebra.

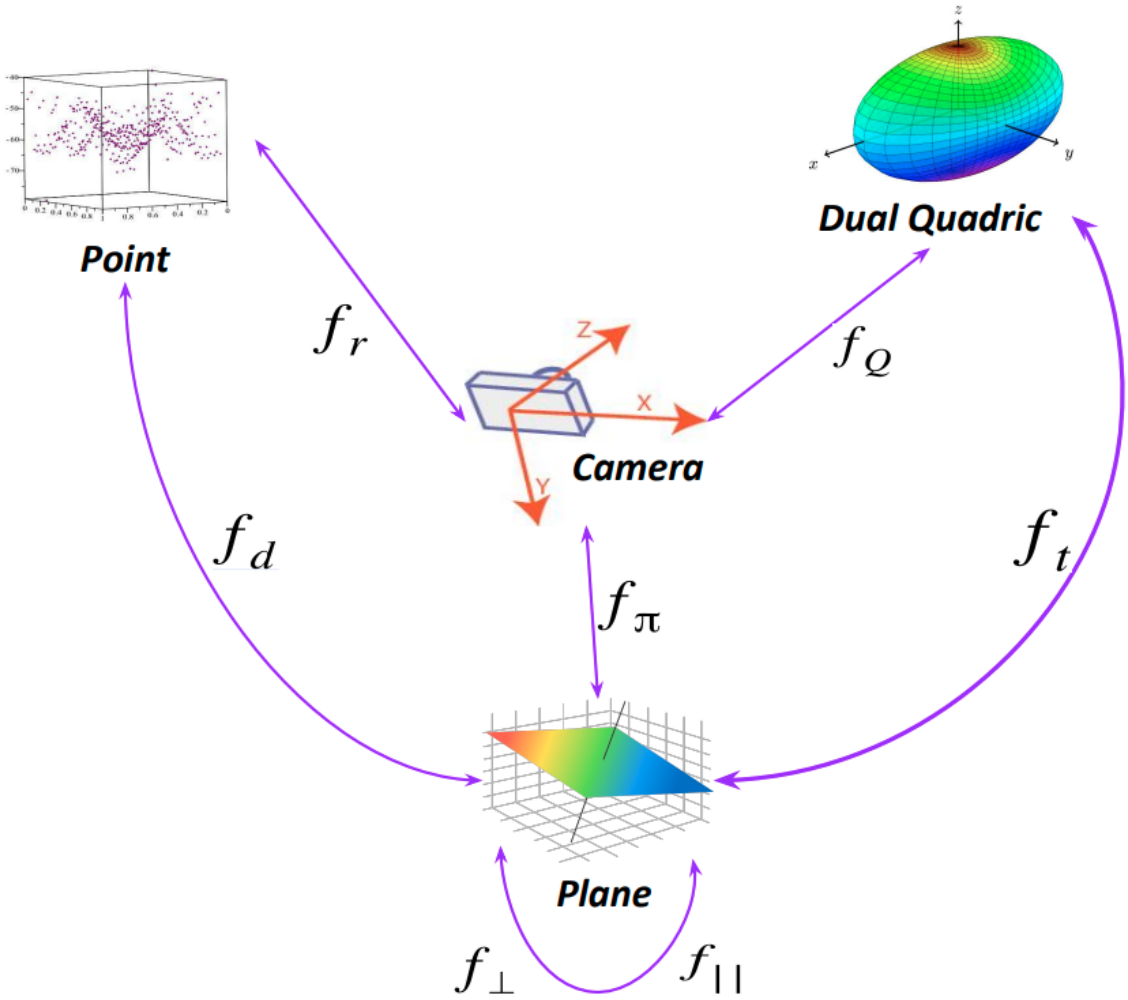

Figure 4.16: Factor graph containing points, planes and objects [12]

- The above figure 4.16 shows the factor graph containing the nodes/ variables representing camera pose, 3D points, quadric parameters, plane parameters that need to be estimated and the connecting edges which represent 7 different types of factor constraints($f_r, f_Q, f_\pi, f_d, f_t, f_\parallel, f_\perp$).
- **1. Observation of points(f_r):** The 3D points observed by the camera at a particular pose is to be registered within the factor graph. The equation tries to minimize the reprojection error.

$$f_r\left(\mathbf{x}_w, \mathbf{T}_c^w\right) = \left\|\mathbf{u}_c - \Pi\left(\mathbf{x}_w, \mathbf{T}_c^w\right)\right\|_{\mathbf{\Sigma}_r} \tag{4.7}$$

In the above equation 4.7, x_w represents the 3d point in world coordinates, T_c^w represents the transformation matrix of the pose of the camera w.r.t the world that can map the observed point in

the current pose c to the world coordinate system. The error is calculated between the pixel location of the point u_c in the current pose c and the reprojected point from the world coordinate into the camera frame using the function $\Pi()$. The error function is the Mahalanobis norm $\mathbf{x}^T\mathbf{\Sigma}^{-1}\mathbf{x}$ where Σ is the uncertainty matrix associated with the factor. Mahalanobis norm takes the covariance structure of the data into consideration while reducing the reprojection error where the distance to the distribution is utilized instead of the distance to a single point as in the euclidean norm.

- **2. Observation of objects(f_Q):** The objects in this case are the ellipsoids. So need to reduce the reprojection error between the conic of the viewed object and the reprojected conic from the ellipsoid in the world cordinates at a particular camera pose c. More details on the conic equation formation in mentioned in the above section on QuadricSLAM.

$$f_Q\left(\mathbf{Q}^*, \mathbf{T}_\mathbf{c}^\mathbf{w}\right) = \left\|\mathbf{C}^* - \mathbf{C}_\mathbf{obs}^*\right\|_\mathbf{F} = \sqrt{\mathbf{Tr}\left(\left(\mathbf{C}^* - \mathbf{C}_{\text{obs}}^*\right)\left(\mathbf{C}^* - \mathbf{C}_{\text{obs}}^*\right)^\mathbf{T}\right)} \tag{4.8}$$

In the above equation 4.8, the norm being used is Frobenius norm. It is measuring the magnitude of the matrix or in other words the root of summed squares of the elements of the matrix. Can be used to check for residuals. Since we are trying to reduce the reprojection error, ideally the value should be 0 or close to 0.

- **3. Observation of planes(f_π):** The distance between observed plane π_{obs} at a particular camera pose c and the plane parameters in the world coordinate π projected into the camera frame is minimized. Since the normal vector n is used to describe the plane, the distance measured is based on the rotational distance in rotation space between the normal vector for π and π_{obs} which is explained in the work by Kaess [9].

$$f_\pi\left(\pi, \mathbf{T}_\mathbf{c}^\mathbf{w}\right) = \left\|d\left(\mathbf{T}_c^{w-T}\pi, \pi_{obs}\right)\right\|_\Sigma^2 \tag{4.9}$$

- **4. Point-plane constraints(f_d):** If there is a certainty that a point lies on a plane, then the constraint between the point and the plane can be established as minimizing the orthogonal distance between the normal vector n representing the plane and a vector formed between the point x and a random point x_o on the plane.

$$f_d(x, \pi) = \left\|\mathbf{n}^T\left(\mathbf{x} - \mathbf{x}_o\right)\right\|_\sigma^2 \tag{4.10}$$

In the above equation 4.10, the dot product between the two vectors is taken. The normal vector n is perpendicular to the plane surface and if the point x is on the plane surface, then the vector connecting x and x_o would be perpendicular to the normal vector and the dot product would be 0.

- **5. Supporting plane constraints(f_d):** In the real world, all the objects on the floor or on the walls are supported by a plane. For example, a clock is supported by a wall plane and a computer is supported by a table plane. This knowledge is exploited to create a constraint between the object

and the supporting plane. The same equation which was used to define dual quadrics, i.e. a quadric is enclosed by tangential planes is used here also.

$$f_t\left(\pi, \mathbf{Q}^*\right) = \left\|\pi^T \mathbf{Q}^* \pi\right\|_\sigma^2 \tag{4.11}$$

- **6. Plane-plane constraints($f_\parallel, f_\perp$):** Based on the Manhattan assumption, 2 planes can either be perpendicular or parallel.

$$\begin{aligned} f_\parallel\left(\pi_1, \pi_2\right) &= \left\|\left|\mathbf{n}_1^\top \mathbf{n}_2\right| - 1\right\|_\sigma^2 \quad \text{for parallel planes} \\ f_\perp\left(\pi_1, \pi_2\right) &= \left\|\mathbf{n}_1^\top \mathbf{n}_2\right\|_\sigma^2 \quad \text{for perpendicular planes} \end{aligned} \tag{4.12}$$

In the above equation 4.12, the dot product between the normal vectors of plane 1 and 2 is taken. In case of parallel planes, the dot product would be 1 and the error term would be 1-1=0 and in the case of perpendicular planes, the dot product would be 0.

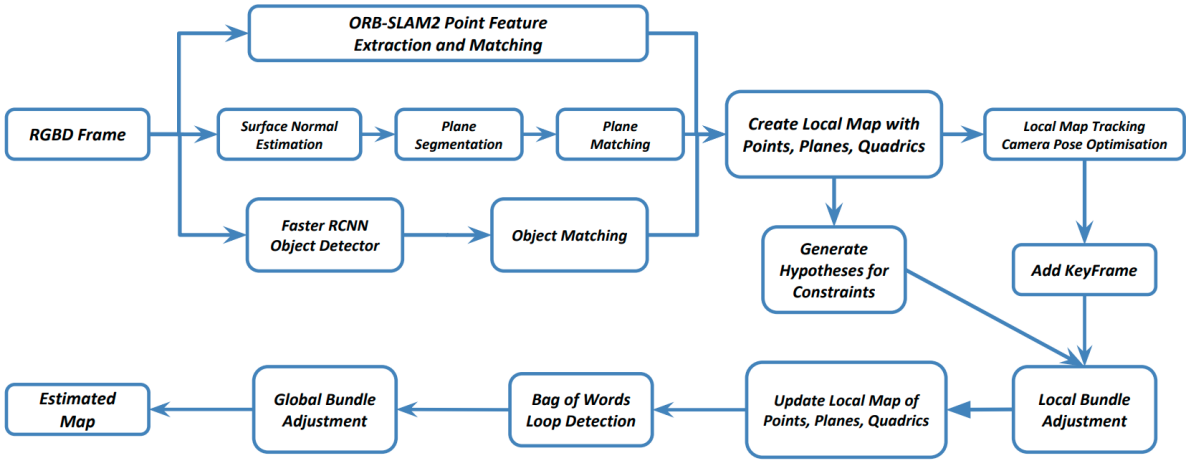

Figure 4.17: SLAM pipeline [12]

- The above figure 4.17 represents the internal pipeline of the slam. This architecture is based on ORB-SLAM except for the fact that the plane and object detection is added in parallel to the point detection at the input side of the pipeline. The optimization step happens in an incremental fashion whenever a new keyframe is added along with its observations (basically an input image and the observed objects, planes and points). Loop closures are detected based on ORB feature matching using the bag of words method as in ORB-SLAM. The input is an RGBD image instead of an RGB image in ORB SLAM for the purpose of plane detection and object quadric initialization. The authors also plan to remove the use of RGBD images and use monocular RGB images in future work to perform depth estimation and semantic segmentation on single images.

- **1. Observation of points:** This is the same as in the ORB-SLAM. Unique ORB features are identified, tracked and matched(data-assosciation) between images. The depth initialization for these points can be made available from the depth channel if an RGBD image is provided as input or can estimate the depth between consecutive RGB images.

- **2. Observation of objects:** A pre-trained Faster-RCNN is used to generate the bounding boxes through object detection. The conic is fitted into the bounding box as explained in the previous section on QuadricSLAM. To deal with noisy detections, the object is initialized only if it is having a confidence of above 95% for a class label. Also to solve the data association problem if multiple copies of the same object are present, a nearest neighbour approach is used to find whether they are 2 separate objects or inconsistent detection of the same object.

- **3. Observation of planes:** Usually planes are detected using RANSAC which not be sufficient to meet the runtime requirements in SLAM to perform online operations. Also we need a finite boundary for the planes instead of infinite plane representation.

- Trevor et.al [14] utilizes the availability of organized point clouds(2D image with depth channel as compared to LIDAR point clouds) to perform segmentation which can reduce the time taken for neighbourhood searching step in unorganized point clouds. Each pixel is assigned a label and 2 pixels can have the same label if they are similar. In the first pass, the first row and first column of the image point cloud are assigned labels based on their similarity with immediate neighbours. After that, for each other pixel, its top and left neighbours are compared for similarity. If similarities are detected, then in the second pass of the algorithm, the labels are merged. To detect planar surfaces from these point clouds, for each point belonging to labels having a large surface(corresponding to floor, wall, ceiling), a surface normal is computed to represent the plane equation. The fourth plane component d is also computed using the dot product of the surface normal and the point's coordinate. Then the angular distance(dot product) between the surface normals and the L1 norm of the d distance parameters of the 2 points as the similarity factor to identify points belonging to a connected plane based on certain thresholds. Since smooth curved surfaces are also getting detected through this method, a max allowable curvature threshold is also set. To identify large surfaces, the min inlier point threshold is set. Later a plane refinement step is also performed to get a less noisy boundary by taking in unsegmented boundary pixels also. The authors also mention that the colour could be also used as a similarity measure by comparing in the Euclidean space.

- For data association in the factor graph, all planes are considered as the number of planes in an environment is assumed to be sparse and also the viewpoint change of the planes between the subsequent image frames is assumed to be less. The data association can be performed by comparing the normal vectors and distance parameters of the plane equations.

- **4. Point-plane constraints:** After performing the plane detection, the inlier points are detected by comparing the distance of the point from the camera with a threshold value. This is because the

farther the point is from the camera, then the depth will have higher uncertainty. If it satisfies the inlier condition, then it is added to the factor graph as a point-plane constraint.

- **5. Supporting plane constraints:** The supporting infinite plane for the object is identified by comparing the orthogonal distance of the centroid of the object quadric with the plane. If it is less than a threshold defined by $max(20cm, a, b, c)$, then the object is supported by the plane. a, b, c is the radius of the ellipsoid and hence the threshold is dependent on the size of the quadric.
- **6. Plane-plane constraints:** For establishing plane-to-plane constraints, every plane is taken into consideration(due to the sparsity of the planes) and a parallel or perpendicular constraint is established if the angle difference between the normals of the plane is within a certain window range. The uncertainty for this constraint is set to high so that the factor graph won't force them to be always perpendicular or parallel but act as a good prior for relative orientation between the planes.
- In the evaluation part, a qualitative comparison is performed as we don't have the ground truth mapping data available for the TUM-RGBD dataset. In quantitative comparison, only RMSE Absolute Trajectory Error (ATE) is estimated. The qualitative comparison is performed because the real world cannot be exactly and semantically mapped for the ground truth. So the best solution is to create a virtual environment in simulators like Gazebo or frameworks like BenchBot(link).

4.2.2 Summary

- The OA-SLAM [15] stands for Object Aided SLAM which utilizes the objects as a key feature for aiding mapping and camera relocalization. It is an improved version of quadric SLAM where the feature points within the environment are also mapped along with the quadric shapes(ellipsoids, cuboids) to improve object tracking and pose recovery in case of tracking failures during sudden motions.
- This method is built on top of ORB-SLAM2. ORB-SLAM utilizes visual bag-of-words keypoint descriptors to compare the ORB features in the current scene with the reference map of the environment. The disadvantage is its restricted invariance to viewpoint changes which makes it difficult to localize when some landmark points are not visible in the current image frame.
- The low-level landmark points are combined with the quadrics of the object generated through object detection methods to form high-level landmarks where objects can be used as anchors for mapping and localization. This can help to improve the viewpoint invariance.
- Even though the representation of the environment with the help of key points helped in efficient computations in ORB-SLAM, it lacked the semantic meaning which could be useful for relocalization in a dynamic environment.
- Previous works on sparse, dense and semi dense
- Previous work on quadric parameters estimation from bounding boxes of object detections.

- Previous work on initial quadric parameter estimation.
- Previous work on camera pose estimation utilizing objects using a pre-built object map.
- Previous work on semantic segmentation on point cloud as a post-processing step to generate dense object maps. Cannot be used for localization as its a post-process step.
- Previous work of QuadricSLAM [4] was mentioned and the disadvantage was the assumption of the data association is solved.
- Previous works on fitting a predefined CAD model onto the object once it is detected.
- Previous work focuses on dense point cloud mapping of objects whereas we focus on an approximate representation of the object properties in terms of position, size and orientation that could be used in most of the applications except where manipulation of the object is needed.

4.2.3 Code Explanation

Pangolin

Ceres

4.2.4 Key insights

Benefits

- Useful in AR applications where the objects and points can be used to relocalize the camera pose when the camera tracking fails.
- Virtual objects can be placed in the real world over the objects identified during the SLAM.
- The proposed approach require only RGB camera instead of RGB-D camera which is very helpful in deployment in devices like mobile phones.
- The object mapping and camera pose is estimated on real time.

Challenges

4.3 Comparative Evaluation of SLAM pipelines

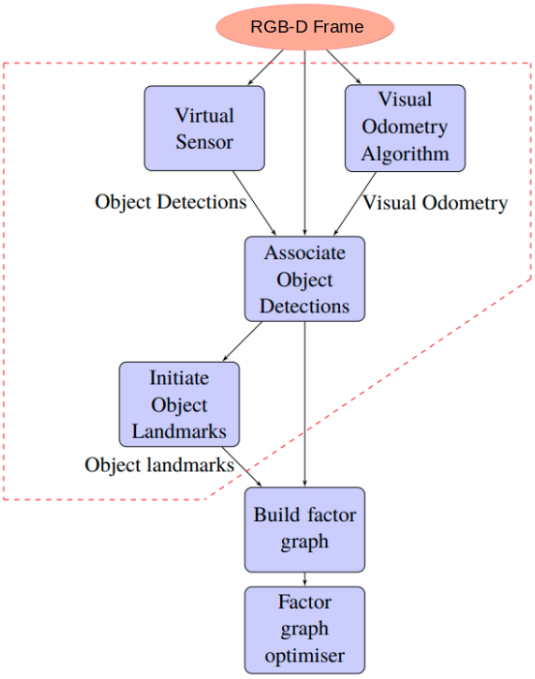

Figure 4.18: Quadric SLAM pipeline [3]

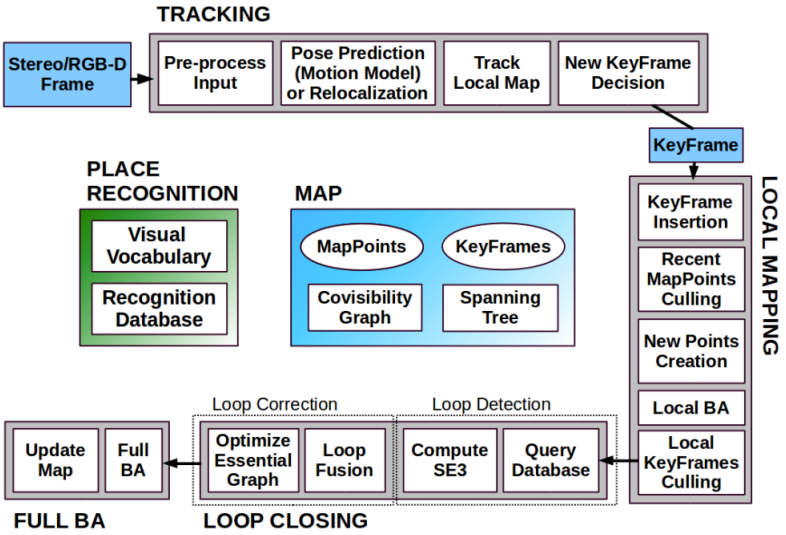

Figure 4.19: ORB-SLAM2 pipeline [16]

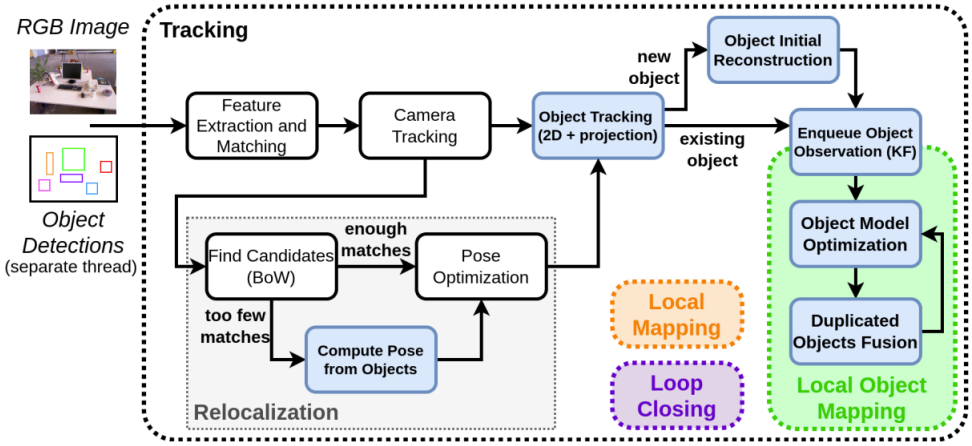

Figure 4.20: OA-SLAM pipeline [15]

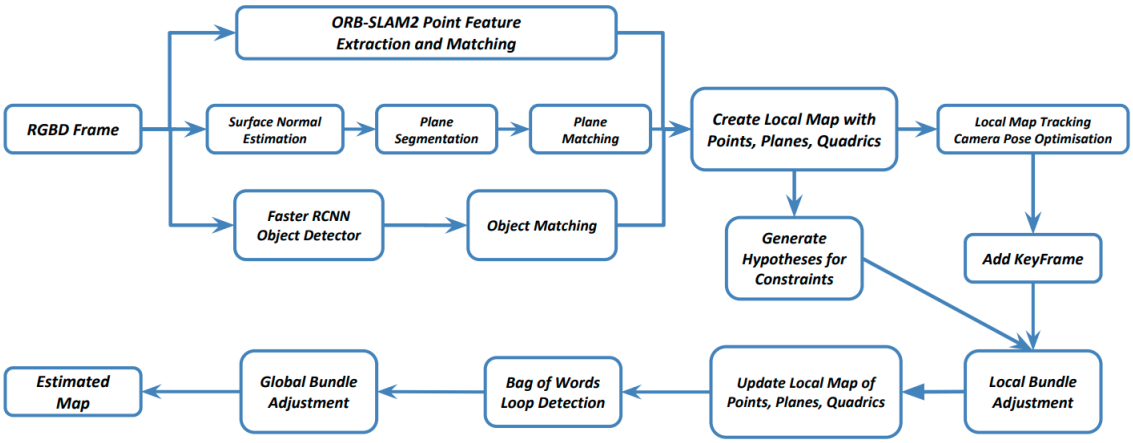

Figure 4.21: Structure Aware SLAM pipeline [12]

5

Evaluation and Results

5.1 Experiment Description

Describe the experiments/evaluation you are performing to analyse your method.

- Short note on the experiment setup

- Short note on the evaluation metrics

- The folder structure

- We are using BOP YCBV dataset(BOP YCBV) for our evaluation purpose as we have ground truth information about the object pose and the camera pose. We will be performing the evaluation on test scene 000048 of BOP YCBV dataset. There are only 5 unique objects in the scene and there are 2243 camera poses and images.

Figure 5.1: Sample image from Scene 000048 of BOP YCBV dataset

- In BOP YCBV dataset, there are RGB and depth images. Also, 3 json files are present. scene_gt.json contains the object poses in terms of rotation and translation matrix for each object in a particular image. scene_camera.json contains the intrinsic and extrinsic parameters of the camera in each image. scene_gt_info.json contains the bounding box parameters for each object in each image. The bounding box parameters are in the format (x, y, width, height) where x,y is the top left corner. More details about the dataset format is given in the project website.(format)

Iterative optimization

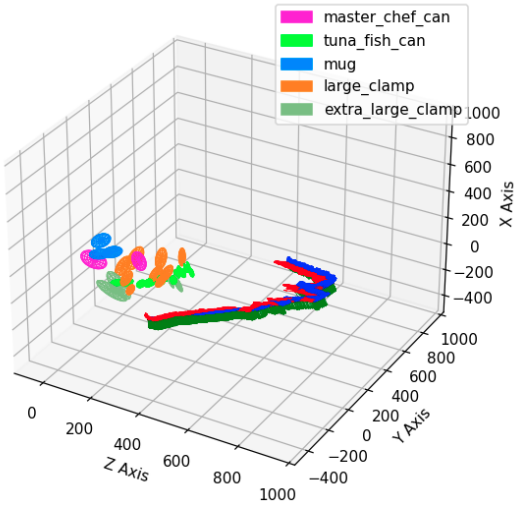

Figure 5.2: Iterative optimized trajectory and object ellipsoids

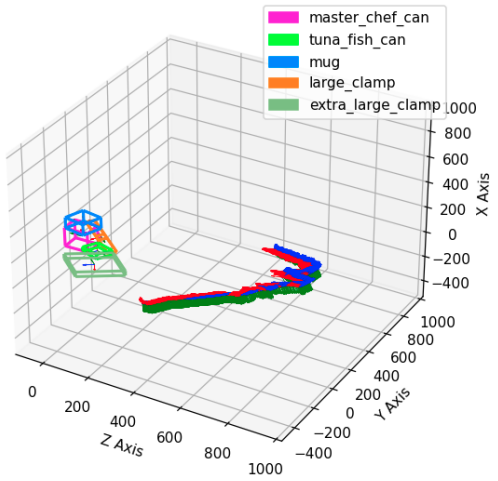

Figure 5.3: Ground truth trajectory and object 3D box

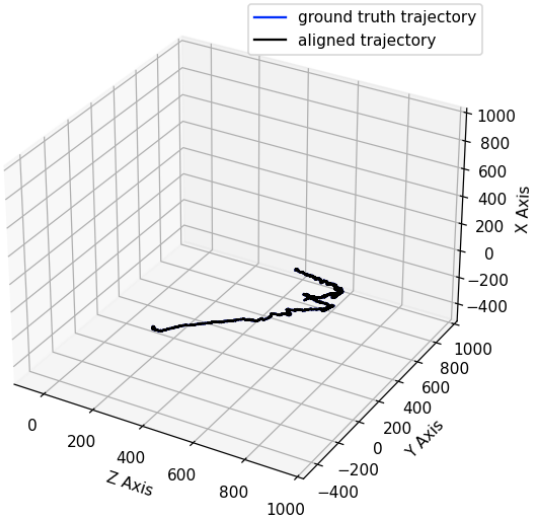

Figure 5.4: Ground truth and estimated aligned trajectories

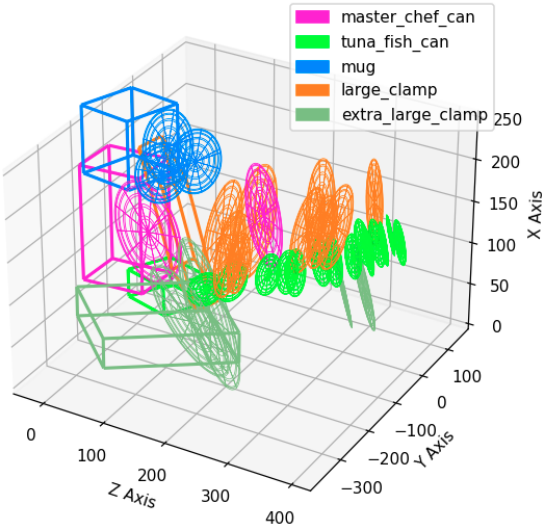

Figure 5.5: Ground truth and estimated object pose

- The above plots show the QuadricSLAM qualitative performance when the iterative optimization option is turned ON.
- In figure5.2, the trajectory and the object poses are plotted. The B,G,R colors of the quiver axis

of the trajectory corresponds to X,Y,Z axis direction. So in this case, the red arrows are pointed towards the objects. The objects are plotted as ellipsoids. We can see there are duplicate instances of the same object even though only 1 object of each class was present in the scene.

- In figure5.3, the ground truth trajectory is plotted along with the ground truth objects. The YCB object model is used to find the length, width and height of the object which is used to plot the 3D box here.
- In figure5.4, we can see that the ground truth trajectory and the estimated trajectory are aligning as the noise model is less noisy.
- In figure5.5, the ground truth object is represented as 3D boxes and the estimated object poses are represented as ellipsoids. We can see that there is association problem existing causing duplication of objects.
- We can see that the objects are getting duplicated over time. This is due to the fact that in each optimization step, the camera poses and the object dual quadric matrix are jointly corrected. This causes the camera poses to deviate heavily to correct the object pose error even though we provide accurate camera poses to the SLAM system by passing the ground truth trajectory. So in the next upcoming steps, the camera assumes to view the same object at a different object pose causing a duplication of the same object. This experiment shows the necessity of a more robust and stable feature detector to run in the backend to estimate the camera pose and object pose accurately which is solved by OA-SLAM which has ORB feature tracking based ORB-SLAM2 running in the backend.

Batch optimization

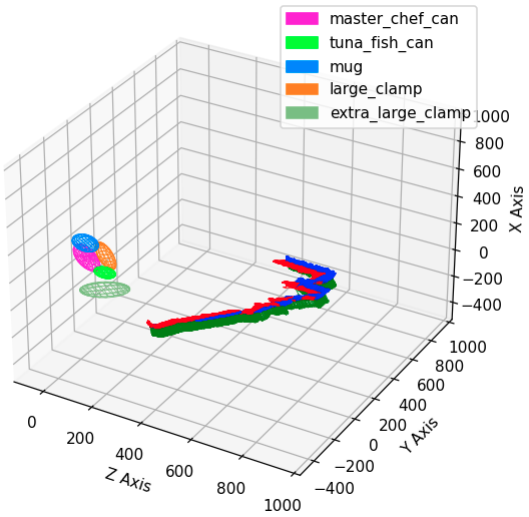

Figure 5.6: Batch optimized trajectory and object ellipsoids

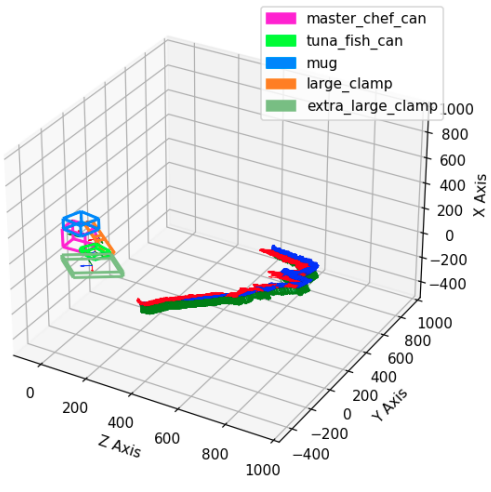

Figure 5.7: Ground truth trajectory and object 3D box

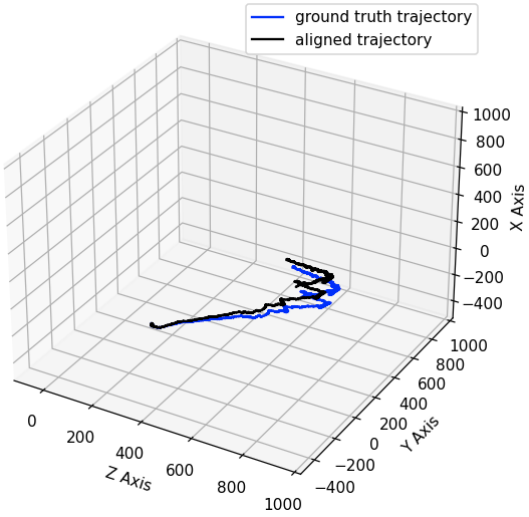

Figure 5.8: Ground truth and estimated aligned trajectories

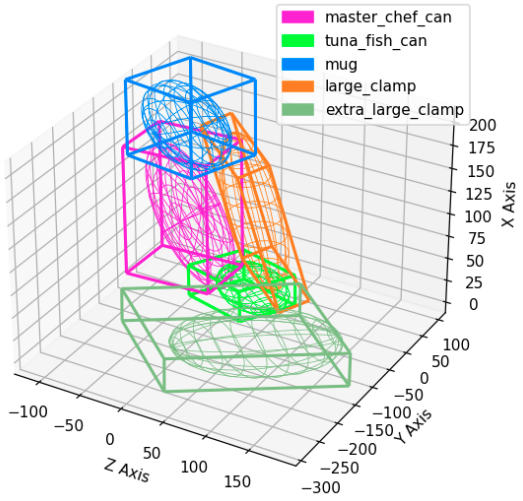

Figure 5.9: Ground truth and estimated object pose

- The above plots depict the QuadricSLAM qualitative performance when the batch optimization option is turned ON.
- In figure5.6, we can see the trajectory pattern and the object poses are similar to what is expected in figure5.7 which is the ground truth.
- In figure5.8, we can see that the trajectories are similar in pattern, but an alignment error accumulates over time.
- In figure5.9, the 3D ground truth boxes and the estimated object ellipsoids are well overlapping. There are no association or duplication issues.
- In cases where we need to test the mapping capability of the SLAM system, we can use the ground truth trajectory and add it to the factor graph with noise model as zero. This makes the odometry variable unmodifiable in the factor graph. This implementation is used to visualize the QuadricSLAM performance for object mapping given the exact camera pose. In such case, the estimated trajectory would align with the ground truth trajectory as in figure5.4.

5.2 Results

Describe the results of your experiments in detail.

- All the plots, pictures, tables
- Rainfall plot
- **EVALUATION METRICES**

Class name	Euclidean error(mm)	Rotation error(rad)
master chef can	38.656	2.187
tuna fish can	40.259	1.417
mug	31.222	1.815
large clamp	16.719	1.850
extra large clamp	73.906	2.043

Table 5.1: Object pose errors

- **Object pose errors**

  The Root Mean Square Error is the average of all the Euclidean errors which is **40.153 mm**. The average rotation error is **1.862 radians**.

- **Object Overlapping Volume Error**

Class name	Overlap(%)
master chef can	24.37
tuna fish can	24.90
mug	48.80
large clamp	67.57
extra large clamp	16.32

Table 5.2: Object Overlapping Percentage

  The average overlapping between ground truth cuboid and estimated ellipsoids is **36.39%**. The higher the volume, the better the overlapping. To increase the accuracy of overlapping checking, increase the number of Monte Carlo samples being generated.

- **Camera pose or trajectory errors**

  – **Trajectory deviation error**

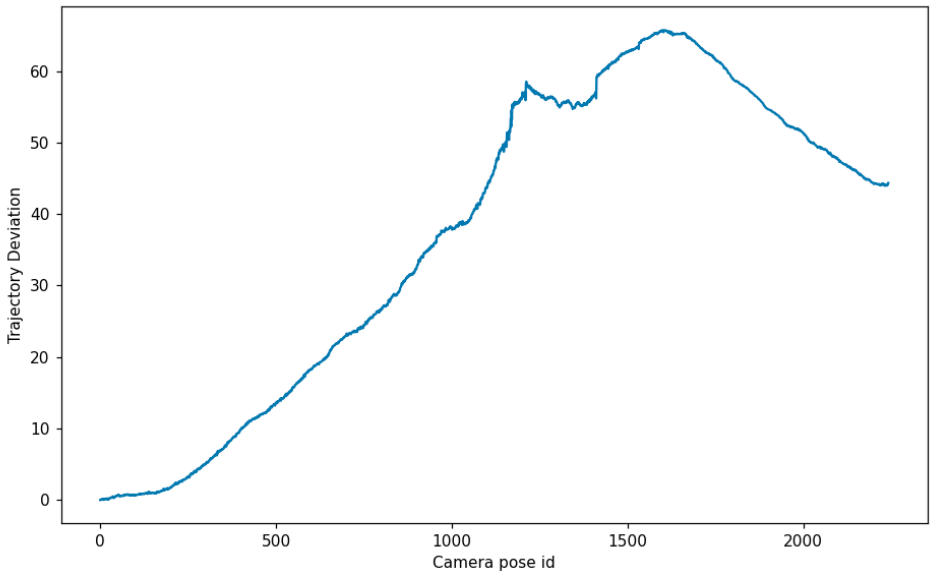

Figure 5.10: Trajectory Deviation Error

The above figure shows the growth of the trajectory deviation over time. Initially, the deviation was around **0 mm** and later reached a maximum deviation of **65.727 mm**. The Root Mean Square Error(RMSE) is **36.922 mm**.

– **Rotation error**

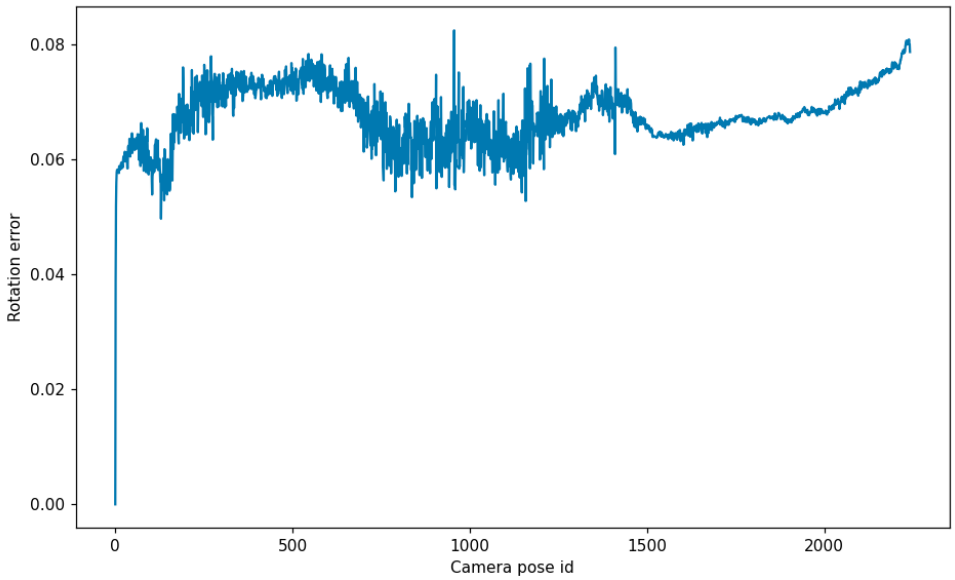

Figure 5.11: Rotation Error

The above figure shows the growth of the rotation error over time. The average rotation error is **0.067 radians**. The minimum rotation error is **0 radians** and the maximum rotation error is **0.082 radians**.

- **Procrustes Analysis** - The estimated disparity value is **0.000235**. Procrustes analysis tries to align two given trajectory points and minimize the distance between them. The disparity or distortion after aligning is returned as the disparity value which indicates a better similarity between the trajectories if the disparity value is low.
- **Fréchet Distance** - The estimated Fréchet Distance is **65.298 mm**. Fréchet Distance takes the shape of the trajectory curve along with its temporal feature to identify the length of the minimum leash distance that can connect two similar points of each trajectory. It is similar to dynamic time warping. A lower Fréchet Distance indicates more correlation or similarity between the two trajectory curves and a higher Fréchet Distance indicates dissimilarity. This value is similar to the maximum trajectory deviation value.
- **Chamfer Distance** - The estimated Chamfer Distance is **62.787 mm**. Chamfer Distance is a symmetric matrix as it computes the Euclidean distance of a point in one trajectory to the neighbouring point in the other trajectory and vice versa. The Chamfer Distance indicates the alignment distance required to make the trajectories similar. Lower Chamfer Distance indicates better similarity.
- **Uninitiated objects error** - The value is 0 as all objects got initiated.
- **Association error** - The value is 0 as all 5 objects are associated correctly.
- **Duplication error** - The value is 0 as there are no duplicated objects.
- **Size of stored map** - For the scene with 2243 camera poses and 5 objects, the file size is 690 KB. This size can further go down by removing the last row of the pose matrix which is always [0,0,0,1].
- **RAINFALL PLOTS OF BOP YCBV TEST SCENES**

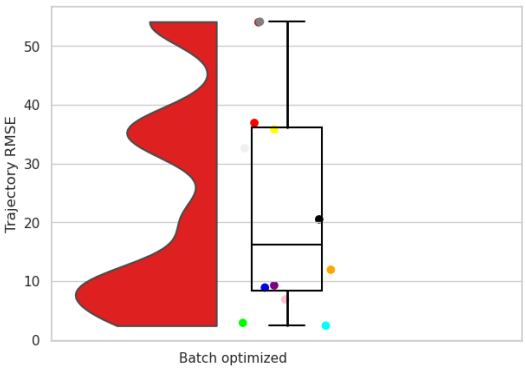

Figure 5.12: RMSE - Batch Optimised

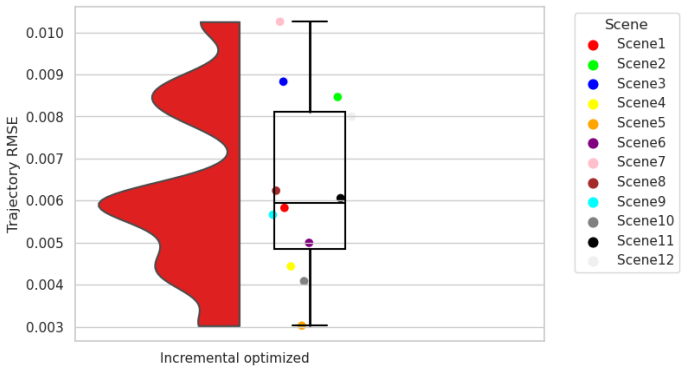

Figure 5.13: RMSE - Incremental Optimised

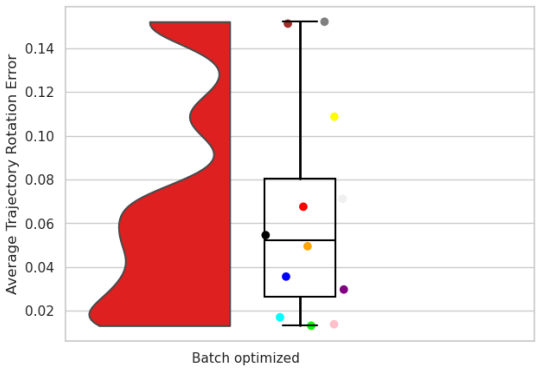

Figure 5.14: Average Trajectory Rotation Error - Batch Optimised

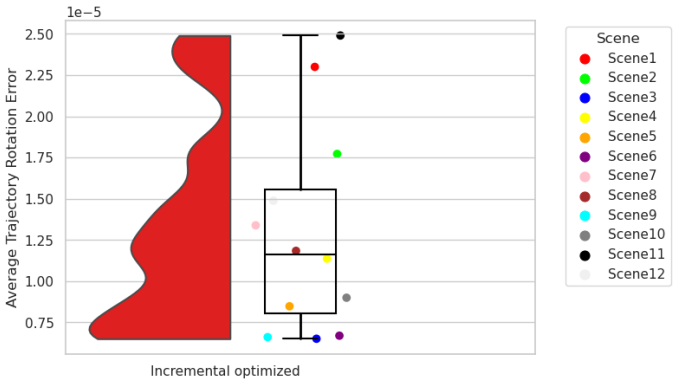

Figure 5.15: Average Trajectory Rotation Error - Incremental Optimised

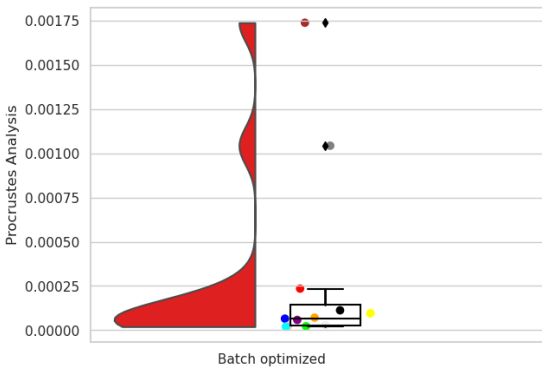

Figure 5.16: Procrustes Analysis - Batch Optimised

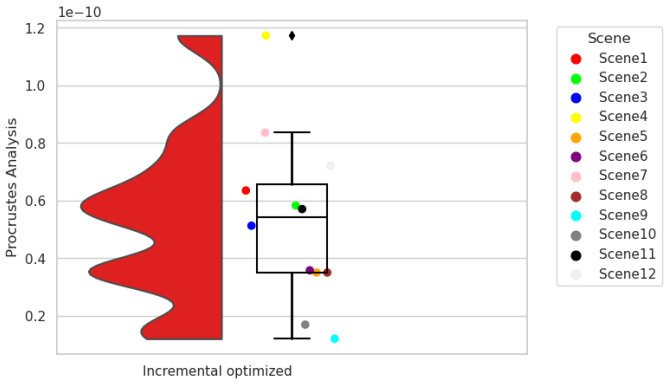

Figure 5.17: Procrustes Analysis - Incremental Optimised

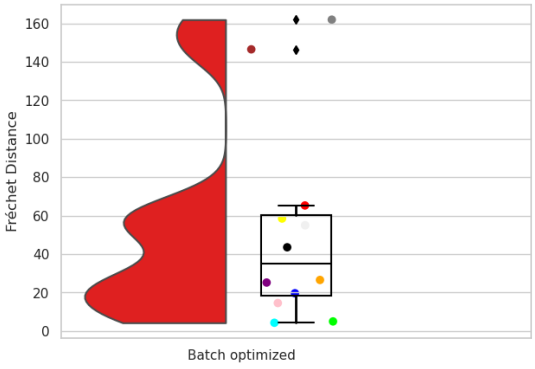

Figure 5.18: Fréchet Distance - Batch Optimised

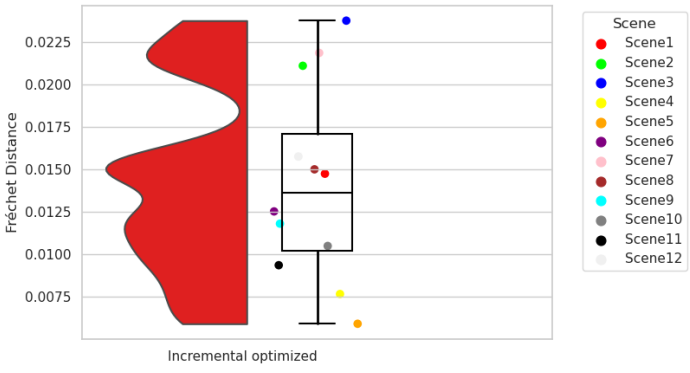

Figure 5.19: Fréchet Distance - Incremental Optimised

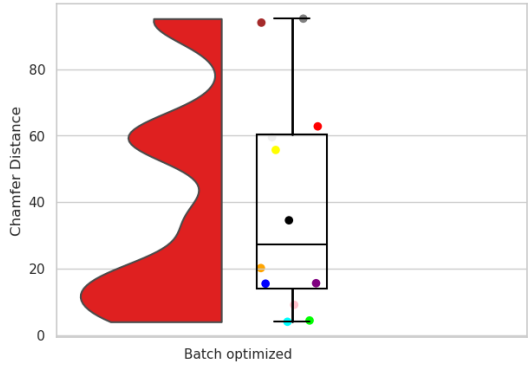

Figure 5.20: Chamfer Distance - Batch Optimised

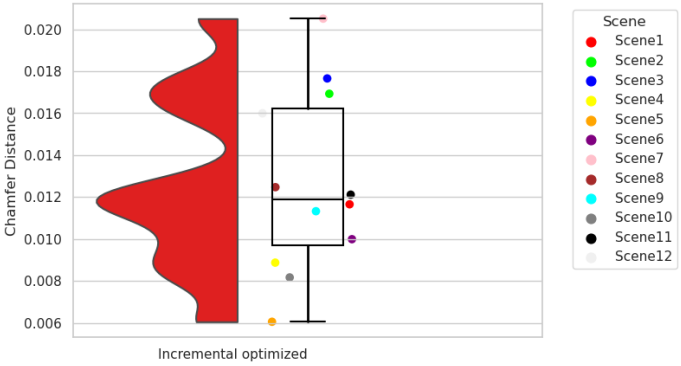

Figure 5.21: Chamfer Distance - Incremental Optimised

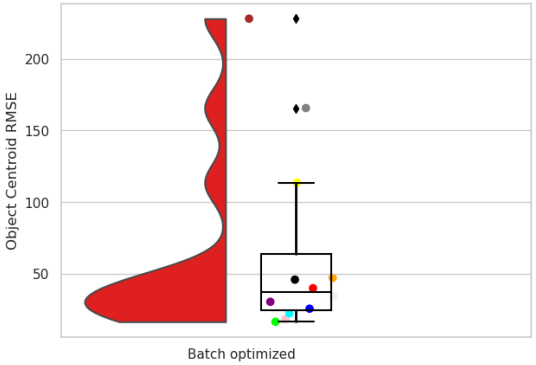

Figure 5.22: Object Centroid RMSE - Batch Optimised

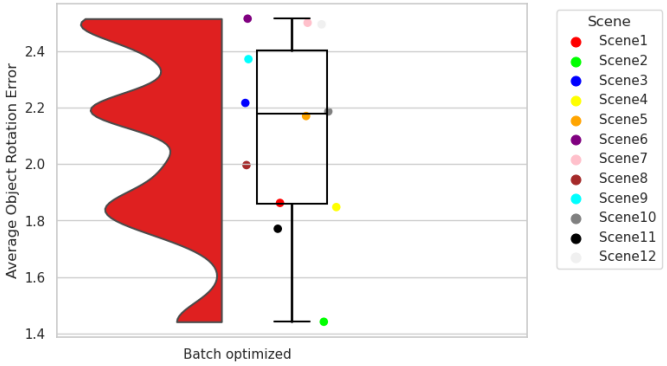

Figure 5.23: Average Object Rotation Error - Batch Optimised

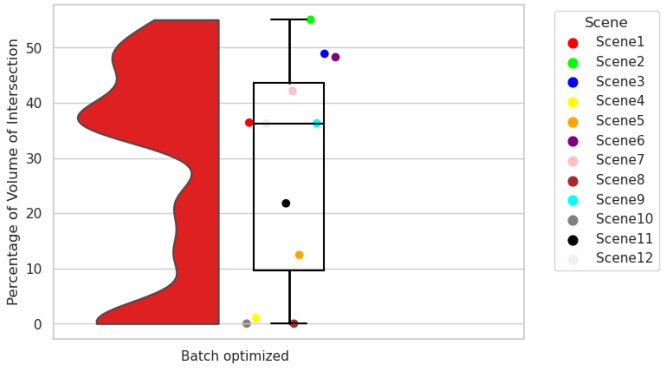

Figure 5.24: Percentage of Volume of Intersection - Batch Optimised

6

Conclusions

6.1 Contributions

- Identified crucial problems and areas of concern
- Performed comparative evaluation of some of the properties.
- Propose some suggestions.

6.2 Lessons learned

- Cause of issues
- Where all failure can happen
- Can object constrain improve the mapping?

6.3 Future work

- Implementation of additional constraints like orb points, planes, objects, and lines.
- Creation of digital twin using CAD model for each object.
- Improved localization using the knowledge of the objects.
- Improved localization based on textual detection.
- Autonomous navigation for SLAM based on exploration and exploitation rather than manual control.
- Performing semantic SLAM in an environment with unknown objects.

A

Design Details

Your first appendix

B

Parameters

Your second chapter appendix

References

[1] J. Sturm, N. Engelhard, F. Endres, W. Burgard, and D. Cremers, "A benchmark for the evaluation of RGB-D SLAM systems," in *2012 IEEE/RSJ International Conference on Intelligent Robots and Systems*, Oct 2012, pp. 573–580.

[2] N. Sünderhauf and M. Milford, "Dual Quadrics from Object Detection BoundingBoxes as Landmark Representations in SLAM," 2017.

[3] K. Kaminski, "Data association for object-based SLAM," Master's thesis, KTH Royal Institute of Technology, Stockholm, Sverige, 2020.

[4] L. Nicholson, M. Milford, and N. Sünderhauf, "QuadricSLAM: Dual Quadrics From Object Detections as Landmarks in Object-Oriented SLAM," *IEEE Robotics and Automation Letters*, vol. 4, no. 1, pp. 1–8, Jan 2019.

[5] F. Dellaert and G. Contributors, "Georgia Tech Borg Lab - GTSAM," https://github.com/borglab/gtsam, May 2022. [Online]. Available: https://github.com/borglab/gtsam

[6] N. Jablonsky, M. Milford, and N. Sünderhauf, "An Orientation Factor for Object-Oriented SLAM," *ArXiv*, vol. abs/1809.06977, 2018.

[7] R. Mur-Artal, J. M. M. Montiel, and J. D. Tardós, "ORB-SLAM: A Versatile and Accurate Monocular SLAM System," *IEEE Transactions on Robotics*, vol. 31, no. 5, pp. 1147–1163, 2015.

[8] T. Lemaire and S. Lacroix, "Monocular-vision based SLAM using Line Segments," in *Proceedings 2007 IEEE International Conference on Robotics and Automation*, 2007, pp. 2791–2796.

[9] M. Kaess, "Simultaneous localization and mapping with infinite planes," in *2015 IEEE International Conference on Robotics and Automation (ICRA)*, 2015, pp. 4605–4611.

[10] R. F. Salas-Moreno, R. A. Newcombe, H. Strasdat, P. H. Kelly, and A. J. Davison, "SLAM++: Simultaneous Localisation and Mapping at the Level of Objects," in *2013 IEEE Conference on Computer Vision and Pattern Recognition*, 2013, pp. 1352–1359.

[11] J. McCormac, A. Handa, A. Davison, and S. Leutenegger, "Semanticfusion: Dense 3d semantic mapping with convolutional neural networks," in *2017 IEEE International Conference on Robotics and Automation (ICRA)*, 2017, pp. 4628–4635.

[12] M. Hosseinzadeh, Y. Latif, T. T. Pham, N. Sünderhauf, and I. D. Reid, "Structure aware slam using quadrics and planes," in *Asian Conference on Computer Vision*, 2018.

[13] Y. Taguchi, Y.-D. Jian, S. Ramalingam, and C. Feng, "Point-plane slam for hand-held 3d sensors," in *2013 IEEE International Conference on Robotics and Automation*, May 2013, pp. 5182–5189.

[14] A. J. B. Trevor, S. Gedikli, R. B. Rusu, and H. I. Christensen, "Efficient organized point cloud segmentation with connected components," in *In: 3rd Workshop on Semantic Perception Mapping and Exploration (SPME), Karlsruhe, Germany*, 2013.

[15] M. Zins, G. Simon, and M.-O. Berger, "Oa-slam: Leveraging objects for camera relocalization in visual slam," in *2022 IEEE International Symposium on Mixed and Augmented Reality (ISMAR)*, Oct 2022, pp. 720–728.

[16] R. Mur-Artal and J. D. Tardós, "Orb-slam2: An open-source slam system for monocular, stereo, and rgb-d cameras," *IEEE Transactions on Robotics*, vol. 33, no. 5, pp. 1255–1262, 2017.